UPPSALA
UNIVERSITET

October 21st, 2020

Alfreð Aðalsteinsson

Department of Chemistry - Ångström

Reactions of Li-metal electrodes in contact with electrolytes, characterized by surface analysis techniques

MSc. Thesis

Supervisors:

Andrew Naylor – Department of Chemistry

Ming-Tao Lee – Department of Chemistry

Subject specialist:

Maria Hahlin

Examiner:

Christer Elvingson

Acknowledgements

I would like to thank my supervisors, Andrew Naylor and Ming-Tao Lee, for their advice and continuous support in all aspects of my thesis. I have learned a lot from this project and enjoyed working under their supervision to a great extent.

I am also grateful to my coworkers in the Structural Chemistry department (ÅABC) for their advice and support. Furthermore, special thanks to Pushpaka Samarasingha for contributing his time and effort to operate the SEM (Scanning Electron Microscopy) apparatus.

Abstract

In modern times, there is an ever-increasing demand for batteries with higher capacity and longer cycle life, e.g., smartphones, laptops, and electric vehicles. Therefore, research and development for rechargeable batteries is extremely important. Li-metal is the lightest metal ($0.53 g/cm^3$), highly reactive and possesses the highest power and energy density, which makes lithium an ideal element to be used in batteries. The Li-metal as an anode material in a battery has its flaws though. Dendrite formation during cycling is one of the biggest challenges for Li-metal batteries. The dendrites build up unevenly across the electrode surfaces, until Li^+ ions have difficulty passing through and eventually pierce the separator and causing a short circuit. To prevent this phenomenon from happening, a proper strategy must be in place. Proper strategies such as altering the solid electrolyte interphase with certain solvents and additives that could prevent the dendrite formation. This issue was tackled in this thesis by identifying the chemical composition of the interphase that forms from dipping the Li-metal into an electrolyte mixture, which contains solvent, salts and additives that do not react violently with Li-metal. Various decomposition products formed on the Li-metal, which were identified via XPS. Various decomposition products formed in the presence of the lithium iodide additive. Some of these products play a role in extending the lifetime of a Li-metal battery.

Popular science abstract

The demand for devices capable of higher energy storage is substantial. The trend is that larger devices, such as the automobile industry are more drawn to become battery powered than ever before. This demand can be met with enormous amount of research, where funding plays a crucial role. The Li-ion battery is an alternative that has already been incorporated in various electrical devices for quite some time, such as smartphones, drones, vehicles and etc. However, the market is craving for even higher capacity and longer durability batteries. Lithium metal batteries is a possible alternative to meet up with this demand. The upside of lithium metal batteries is that they have approximately 5 times higher capacity than conventional Li-ion batteries. The drawback is that they are not as durable, i.e. the capacity fades more rapidly with each cycle, compared to conventional rechargeable lithium batteries (e.g. Li-ion batteries). This capacity fade is correlated with dendrite formation on the lithium metal surface. A proper strategy must be in place to tackle this issue. This issue was countered in this thesis by identifying the chemical composition of the protective layer that forms on the lithium metal from the electrolyte components. This was done to obtain a greater understanding of what happens on the lithium metal surface before it is used in a battery.

Contents

List of Figures

List of tables

List of Abbreviations

BE	Binding energy
CPS	Counts Per Second
DME	Dimethoxyethane
DMC	Dimethylcarbonate
DOL	1,3-Dioxolane
EDS	Energy Dispersive Spectroscopy
LiBOB	Lithium bis(oxalato)borate
LiTFSI	Lithium bis(trifluoromethanesulfonyl)imide
LiTNFSI	Lithium (trifluoromethanesulfonyl)(n-nonafluorobutanesulfonyl)imide
LTO	Lithium Titanate Oxide
PS	Polysulphide
rGO	reduced Graphene Oxide
SEI	Solid Electrolyte Interphase
SEM	Scanning Electron Microscopy
S/N	Signal to Noise
TEGDME	Tetraethylene glycol dimethyl ether
XPS	X-ray Photoelectron Spectroscopy

1. Background and Theory

Lithium is the lightest metal (density of 0.53 g/cm^3) in the periodic table. It is also one of the most reactive metals and has the lowest electrochemical potential (E^0 = -3.05 V) against hydrogen's standard electrode potential. In batteries it is known to provide very high energy and power density.[47] Lithium is also known for its immense reactivity towards water producing hydrogen gas (H_2) and lithium hydroxide (LiOH), see equation 1:

$$2Li + 2H_2O \rightarrow 2LiOH + H_2 \quad (1)$$

This reaction is exothermic and under certain conditions, the heat becomes high enough to ignite the hydrogen, resulting in an explosion. It is important that the electrolyte consists of nonaqueous solvents with low reactivity towards Li-metal, to prevent a catastrophic event from happening.[47] When lithium reacts with organic solvents, such as carbonate and ether based, it can form protective coatings (SEI = Solid Electrolyte Interphase) on the surface. The role and formation of SEI is discussed in greater details in section 1.2.

One could classify anode materials into three categories: Intercalation, conversion and alloys.[51,52] Li-ion batteries typically exhibit the intercalation type of anodes. During charge/discharge, the host material (e.g. graphite and Lithium Titanate Oxide (LTO)) does not undergo a structural change when the Li^+ ions move in and out of the anode material.[51] Conversion type of materials undergo conversion redox reactions, which ultimately result in a metallic phase being formed,[52]

$$M_xR_y + (y.\ n)A \rightarrow x\ M + y\ A_nR)$$

where, A = Li, Na and M is a transition metal, R = O, S, Se, P or H. However, conversion anode materials have many drawbacks in terms of cyclic stability. Alloy type anodes, Li-Al are among the first to be developed for Li-ion cells. Other metals that alloy with Li are Mg, Sn and Sb. One could classify Li-metal anodes into the alloy category, but a typical alloy would contain at least two metals.[52]

One should not confuse rechargeable lithium batteries (secondary cells) with non-rechargeable lithium batteries (primary cells).[47] Primary Li-metal batteries have higher energy densities, higher voltage, a wider operating temperature range and longer shelf life compared to secondary batteries. They emerged in the 1970s and are known to consist of materials such as Li-I_2, LiCuO, Li-MnO_2 and $Li(CF)_n$. The practical uses of Li-metal primary batteries are mainly in watches, medical devices, calculators and military equipment.[48] However, the secondary Li-metal

batteries have a broader scope of application, since they can be charged repeatedly.[47, 48] Many challenges lie ahead for the secondary Li-metal batteries, such as the dendrite formation. This will be discussed in detail in section 1.1

A battery consists of an anode, cathode, separator, electrolyte and two current collectors, as depicted in **Figure 1**. Aluminum is typically used as a current collector for the anode side and copper for the cathode. The electrolyte plays an important role of carrying the positively charged ions (Li^+ ions in this case) between the two electrode components through the separator. The Li^+ ions are intercalated in the anode upon charge and in the cathode upon discharge. The separator's role is to prevent the electrons from flowing inside the battery.[45, 46]

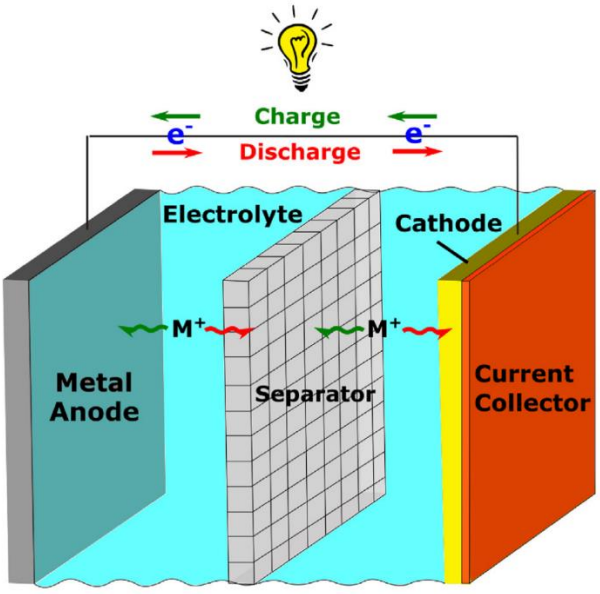

Figure 1: A simplified illustration of how a battery operates during charge and discharge. Reprinted with permission from ref. 46. Copyright © 2019 R.Borah et al. Published by Elsevier Ltd.

When a battery is discharging, the Li^+ ions are released from the anode to the cathode, while simultaneously generating a flow of electrons to power a device. When the battery is being charged, the opposite process occurs. This phenomenon is driven by the potential difference between the electrodes. The cathode releases Li^+ ions to be received by the anode, while electrons are stored in the cathode.[45]

1.1 Li-Sulphur batteries

Li-Sulphur batteries have attracted a lot of attention from the community of electrochemists for over four decades.[1] The Li-S battery system is an enormous leap from the Li-ion, in terms of specific capacity and energy density. Sulphur (S_8) is an abundant mineral in the earth's crust, non-toxic and environmentally friendly. The theoretical capacity for a sulphur cathode, which

undergoes a reduction to Li_2S, is about 1675 mAh/g, along with a relatively low theoretical voltage of 2.24V vs. $Li^+/Li(0)$ and yet still is competitive, in terms of gravimetric energy density (2600 Wh/kg), as a cathode material. Li-metal has also a high theoretical capacity (3860 mAh/g) and as mentioned before, out of all elements it has the lowest electrochemical potential.[1, 2] This high energy storage system is accomplished via a phase-transformation chemistry, whereas the main components are pure sulphur (cathode) and metallic lithium (anode). However, the cycle count of Li-S batteries is known to be low due to the lithium polysulphide's (PSs) shuttle effect, dendrite formation on the Li metal anode interface and volume fluctuations of the sulphur cathode. A strategic approach to minimize the dendrite formation would be to modify the protective layer (SEI) on the Li metal surface. This can be achieved by using electrolyte additives, which will be discussed later. Such an approach is crucial to obtain a cell with high capacity and high Coulumbic efficiency.[3, 4]

There are several reasons why Li-S batteries are not a widespread electrochemical energy storage device. The most noticeable disadvantage with pure sulphur cathodes is that they are highly insulating. Therefore, conductive additives in relatively high quantities are needed, which will decrease the gravimetric and volumetric capacity of the Li-S cell. Another disadvantage would be the solubility of long chain polysulphide (PS). This occurs from reduction of the pure sulphur cathode and/or by oxidation of shorter chain PS. Both processes will degrade the Li-S cell. The anode side, Li-metal, is also affected by these types of parasitic reactions. The PS will be electrochemically reduced once they reach the Li-metal through the electrolyte and cover it with insoluble Li-PS products.[5]

The shuttling effect is a phenomenon that plagues the Li-S battery and causes capacity decay of the sulphur cathode.[6] In a Li-S cell, it is caused by the dissolution of lithium polysulphides (PS) in the electrolyte. The Li ions from the anode will form lithium PS. This process is inevitable but can be decreased with the right approach. Such as from promoting the formation of an SEI (Solid Electrolyte Interface) film, that is formed from liquid electrolyte additives. It has been reported that electrolyte additives with N-O bonds tend to improve the cycle life and Coulumbic efficiency of the Li-S cell. However, there are other promising additives that will be discussed in greater details in section 1.4. When an electrolyte contains $LiNO_3$, it forms a passivation layer (SEI) on the Li metal interface during cycling, to form both inorganic (LiN_xO_y) and organic (ROLi and $ROCO_2$) species. From these layers they effectively decrease the shuttle effect in the Li-S electrochemical system.[6]

1.2 Solid electrolyte interphases (SEI's)

Li-metal reacts with most organic solvents and forms a surface layer (i.e SEI). In a battery, it is crucial to have rapid transport of electrons and ions, in order to obtain high energy density and long lifespan. Therefore, an ideal design of a SEI would be to enhance its ability to conduct Li ions rather than electrons (**Figure 2**a. This will avoid unwanted side reactions on the Li-metal surface and induce an effective improvement of cycling efficiency. The SEI's electronic insulation prevents the Li-metal from reacting with electrolyte derivatives. The thickness of SEI's are typically ~20 nm thick. Its formation consumes the anode and electrolyte, which gradually lowers the cells efficiency[12, 49]

The SEI structure can be described with two broadly accepted models: The mosaic model (**Figure 2**b) and the multilayered model (**Figure 2**c), whereas both have been experimentally confirmed. In the mosaic model there are various reductive decomposition products forming on the Li-metal surface simultaneously, and a mixture of insoluble products that form in multilayers. In contrast, the multilayered SEI model is not homogenous either, in terms of the thickness direction (**Figure 2**c). Inorganic species tend to be in the layer close to the Li-metal surface, such as Li_3N, LiOH, Li_2O and Li_2CO_3. The outer layer film would have the tendency to consist of organic species, such as ROLi, $ROCO_2Li$ and $RCOO_2Li$.[49]

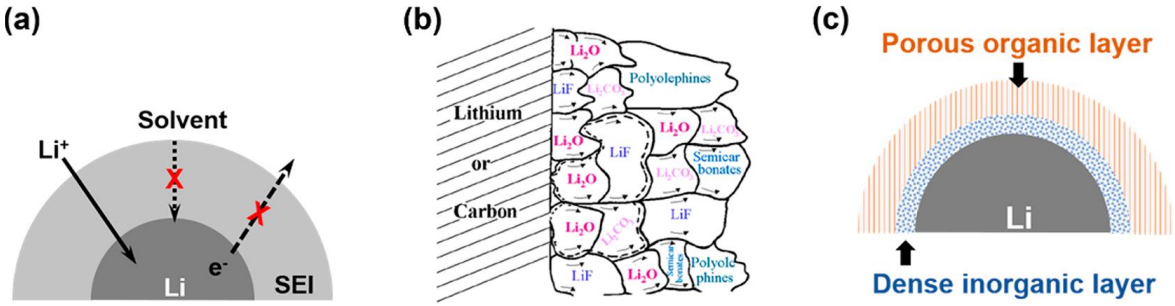

Figure 2: SEI features. a) An ideal functioning SEI with high ionic conductivity and electronic insulation. b) Mosaic SEI model. c) Multilayered SEI model. Reprinted with permission from ref. 49. Copyright © 2018, American Chemical Society.

The inner inorganic layer is what gives a rise to the electronic insulation of the SEI. This is because most inorganic materials that form on the Li-metal surface have extremely low electronic conductivity and can prevent electrons from being transferred from the Li-metal anode to the electrolyte. The mechanism of the ionic transfer in the inorganic layer is not fully understood yet. However, it is believed that the ionic pathways are through grain boundaries and crystal phase.[49]

One should keep in mind that the SEI in this thesis is not the typical type one would exhibit from a battery being cycled. Herein the Li-metal anode was investigated without having been assembled into a battery and cycled. Therefore, one could expect the SEI to look differently, compared to a cycled battery.

1.3 Current "state-of-the-art" Li-metal battery research

Li-metal is in extremely high demand in the field of advanced energy storage. Furthermore, as mentioned before, lithium metal has for a long time been acknowledged as the best alternative anode material, because it has the highest theoretical specific capacity, lowest potential and is light weight (0.59 g/cm^3). However, its drawbacks are the dendrites that form during cycling (**Figure 3**b). This has prevented the advancement of Li-metal-based batteries, ever since the 1980's.[48] The dendrite formation does not only penetrate the separator but can also result in a catastrophic failure of the cell, which is a serious safety hazard. In the subsections below multiple publications will be reviewed, some of which are less related to this work. However, they all focus on decreasing the dendrite formation on Li-metal anodes.

1.3.1 Lithium-Metal Foil Surface Modification

In a publication by J. Becking et al.[50] they investigated the native surface film and the initial surface roughness of Li-metal anodes, in terms of the electrochemical performance. The electrolyte consisted of 1M LiTFSI (lithium bis(trifluoromethanesulphonyl)imide) in TEGDME:DOL (1:1 by volume). They observed that the initial cycles were crucial to be investigated. Since during the first cycles, the initial surface chemical composition and morphology was gradually lost. This happens because fresh lithium is repeatedly (with each cycle) reacting with the electrolyte, resulting in irreversible reactions. The initial Li-metal surface roughness (i.e. surface defects) was critical for the performance of the cell. Applying the roll-press technique removed the surface roughness, which was measured with Atomic Force Microscopy (AFM), resulting in flatter topography and lower concentrations of Li_2CO_3. Such changes had a positive impact on the overpotentials (45 mV lower than for the untreated Li-metal foil) measured during charging/discharging of the cell.[50] Therefore, it is possible that the lower surface roughness of the lithium decreases the dendrite formation.

What was most intriguing about the XPS results was the ratio between the F 1s peaks for LiTFSI salt at 688.8 eV and LiF at 684.9 eV. After 5 cycles the peak ratio (LiTFSI:LiF) was 4:1 for the untreated Li-foil and 2:1 for the rolled one. The amount of LiF was two times higher for the rolled Li-foil, after 5 cycles. It is reported that increased amount of LiF leads to reduced

impedance and extends lifetime of the cell. However, after the 10th and 15th cycle, the ratio was 2:1 and 1:1 respectively.[50]

1.3.2 "Pre-planted nucleation seeds for rechargeable metallic lithium anodes"[7]

In a publication by Liu et al.[7] they demonstrated an effective strategy to accomplish a Li-metal anode with Cu nanoparticles that were pre-planted by using a facile rolling and folding technique. What made it even easier, is the ductility of Li-metal.[8] The main reasons why Cu was chosen as heterogeneous nucleation seeds is that it is known as a prominent current collector material and the fact that Li and Cu are much easier to obtain compared to other noble metals.[9]

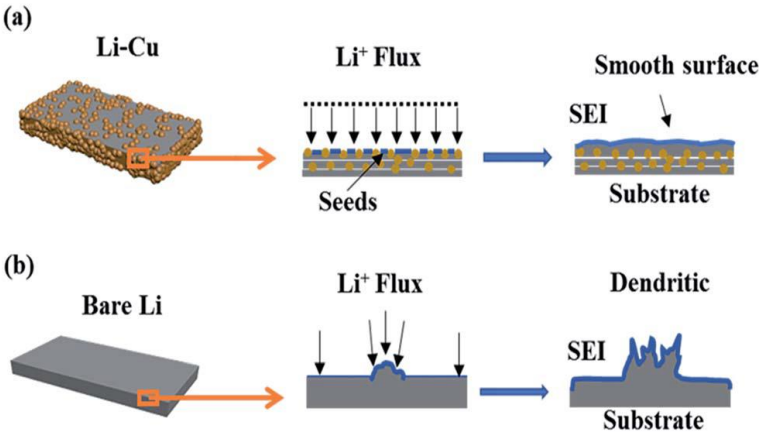

Figure 3: Deposition of Li during cycling on a) Li-Cu hybrid anode and b) bare Li-metal anode. Reprinted with permission from ref. 7. Copyright © 2017, The Royal Society of Chemistry.

Cu nanoparticles were distributed uniformly on the surface and the inside (since Li is rather porous) of the Li-metal anode. The Cu nanoparticles did not only act as nucleation sites, but was also functioning as a prominent inducer for ion flux and electric field while the lithium was being plated (**Figure 3**a). As a result, the Li-Cu hybrid anode along with a $LiFePO_4$ cathode, had a lower over-potential (~38 mV) and a remarkable cycle stability, with a specific capacity of 2023 mAh/g.[7] Furthermore, the dendrite formation was reduced from implementing this method. However, this method has not yet been carried out in a Li-S battery system as far as of today. It would, however, be interesting to see how effective it would be.

1.3.3 Layered reduced graphene oxide (rGO) as host for Li-metal anodes

Carbon-based compounds would be ideal as host materials for Li-metal anodes. Since carbon is the lightest element that can be utilized for scaffold construction. Furthermore, carbon-based materials such as graphene and nanotubes are known to have high surface areas along with being outstandingly robust. The extremes of the redox environment in Li batteries would not

have much effect on the stable carbon materials. Therefore, carbon materials are an ideal candidate to function as an electrode materials and/or a conducting additive.[10]

Reduced grapehene oxide (rGO), see **Figure 4**c, shows characteristics of high lithiophilicity, which is unique and rarely seen among carbon-based materials. When lithiophilicity is high, it indicates that molten Li can be infused to a surface more easily.[10]

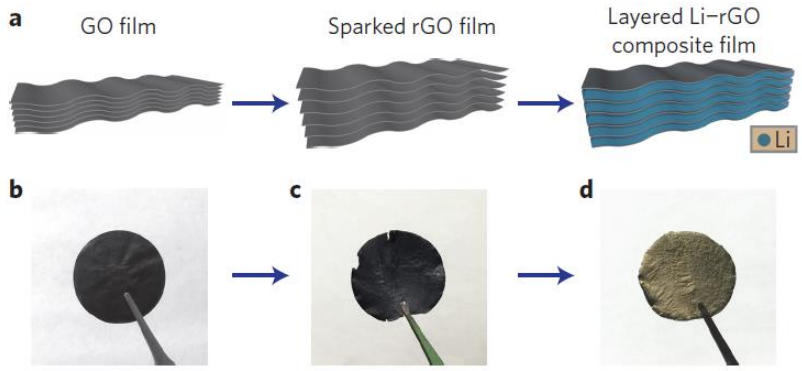

Figure 4: a-d) Graphene oxide film sparked and introduced with Li to form a layered Li-rGO composite film. Reprinted with permission from ref. 10. Copyright © 2016, Nature Publishing Group.

Therefore, a layered rGO film was sparked to create nanopores, which could be infused with molten Li to form a layered Li-rGO electrode (**Figure 4**a). The Li-rGO revealed to be extremely flexible and only a small amount (~20%) of thickness fluctuation to the electrode during cycling. The SEI is stable, even at high current rates (10C), the specific capacity is maintained surprisingly well, compared to the bare Li-metal anode. This design seems to be stable and a viable option for Li anodes in Li battery systems with high energy and power output. Furthermore, it most likely reduces the dendrite formation on the Li-metal.[10]

1.4 Electrolyte components

Electrolytes can be either solid- or liquid-state. The solid-state electrolytes are commonly polymer based. Polymers that fulfil the criterion of high ionic conductivity are few, such as Polyethylene Oxide (PEO). To achieve a highly conductive Li-based polymer involves a comprehensive understanding of ionic dissociation and transport. However, for liquid electrolytes to fulfill this high conductivity criterion, depends on specific dielectric and viscosity constants of the solvents.[51] In this thesis, only liquid-state electrolytes were produced.

An electrolyte additive is a material that improves and/or preserves the battery. An additive could also induce the formation of a more stable SEI, as will be discussed later.

1.4.1 LiTFSI vs. LiTNFSI

LiTFSI in the presence of $LiNO_3$ additive has been reported to not only prevent dissolution of PS in Li-S cells, but also improving the cycling stability of Li-metal anodes.[11] Earlier works on Li-S cells with ether-based electrolytes have mostly focused on LiTFSI (**Figure 5**), due to its high ionic conductivity, electrochemical stability and its ability to form stable SEI layers on the Li-metal anode.[11, 12] However, a similar Li-salt, LiTNFSI (**Figure 5**) (lithium(trifluorosulphonyl)(n-nonafluorobutanesulphonyl)imide), has been reported to be highly electrochemically stable towards the anode and does not exhibit aluminum corrosion at high potentials (3-5 V) vs. $Li^+/Li(0)$, compared to LiTFSI.[13] As of today, this is the only publication about the performance of LiTNFSI in Li-S batteries.[11]

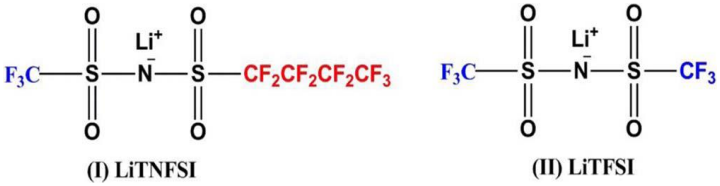

Figure 5: Chemical structures of (I) LiTNFSI and (II) LiTFSI. Reprinted with permission from ref. 11. Copyright © 2013, American Chemical Society.

Cycling experiments were conducted individually on LiTNFSI (1M) and LiTFSI (1M), along with $LiNO_3$ (0.4M) in a DOL:DME (1:1 by vol.) solvent mixture. The initial charge capacity of the respective Li salts were 1219 mA/h and 1132 mA/h. The cycling was conducted at 0.2 C and resulted in a capacity retention rate of 62% and 54% over 400 cycles. One could assume that this great difference would arise from the different Li salts used and could be expected from the different surface chemistry that is taking place on the Li-metal anode, due to the different anionic structures between the LiTNFSI and LiTFSI.[11]

Scanning electron microscopy (SEM) revealed how different anionic structures, of the different Li salts affect the surface of the Li-metal anode. After 50 cycles at 0.2 C charge/discharge rate, with the LiTFSI-based electrolyte, the morphology appears to be rough and irregular. This is possible due to dissolutions and regrowth of the SEI from charging and discharging of the Li-S cell (**Figure 6**d). The Li-metal surface appears, however, to be smoother and more compact (**Figure 6**d) from cycling with the LiTNFSI-based electrolyte. The cross-sectional views (**Figures 6**b, c, e and f) indicate that the Li-metal anode is thicker and denser from the LiTNFSI verses the LiTFSI. This would suggest that the SEI formed in the Li-S battery is more robust than with LiTFSI.[11]

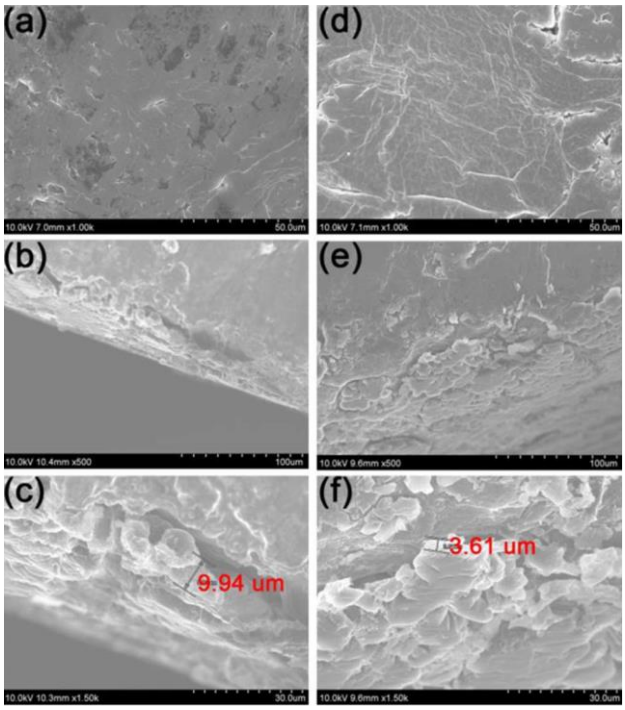

Figure 6: SEM images of the Li-metal anode in a Li-S battery system, after 50 cycles at 0.2 C charge/discharge rate a-c.) From LiTNFSI-based electrolyte. d-f.) LiTFSI-based electrolyte. Reprinted with permission from ref. 11. Copyright © 2013, American Chemical Society.

1.4.2 Lithium Iodide (LiI) as an electrolyte additive

Electrolyte additives, such as LiI and InI_3 have shown remarkable results in forming a stable SEI layer on Li-metal anodes, which in fact has proven to decrease the capacity loss of Li-S batteries after each cycle.[14, 44] This is because the protective layer formed on the electrode's surface prevents dendrite formation. The dendrites could grow to puncture the separator film and eventually causing a short circuit. In terms of cell cycling performance, it is reported that the LiI reduces the overpotential during the first few cycles. This means that the hysteresis between the first charge and discharge is significantly reduced.[14] Additionally, solid-state electrolytes, such as LiI, are known to show high ionic conductivity (10^{-7}-10^{-3} S/cm), which could improve the ionic conductivity of the Li-metal SEI layer.[15]

Quantum chemistry (QC) calculations were conducted (**Figure 7**), in order to gain better insight on the mechanism of how the protective coatings form on the electrode's surface.[14] In this publication the electrolyte components were LiTFSI, LiI and DOL:DME as solvents. The reactivity was examined between the DME/LiTFSI and DME/LiI. Oxidation between DME and I^-, resulted in an exothermic (-75kJ/mol) H-abstraction from DME by I^-. The products were a H^+I^- and DME(H^-) radical (**Figure 7**a). This reaction is expected to happen readily, as long as solvent-separated I^- anions have not been depleted from the electrolyte. The reaction between a $TFSI^-$ anion and DME (**Figure 7**b) was predicted to be endothermic (+15 kJ/mol). Therefore,

these results illustrate that this reaction is considerably less feasible to take place.[14] However, LiTFSI tends to be more dissociative than LiI. Therefore, in theory, the TFSI anions will be more separated in the electrolyte solvents and be more accessible for this type of reaction to take place (**Figure 7**b),[16] even though the energetic is less favorable.

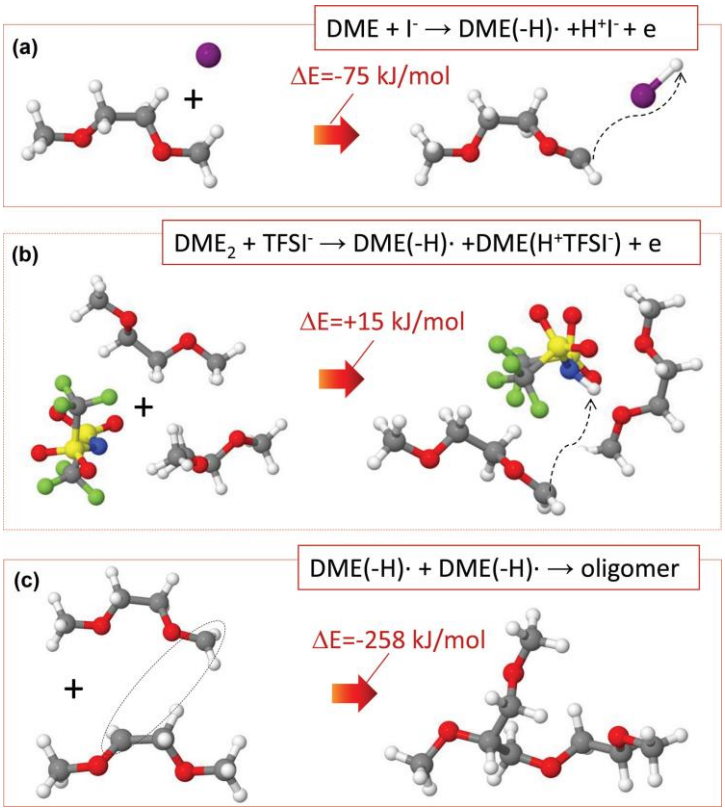

Figure 7: Results of QC calculations and proposed mechanisms of DME and LiTFSI: a and b) the first steps of the decomposition of the DME/LiI and DME/LiTFSI electrolyte components, while DME(LiI·) radical was being reduced and coupled with a) an Oxidation of DME with an I^- anion and b) an oxidation of DME with TFSI anion, resulting in formation of DME(H^-)· radicals; c) Two triplet DME(H^-)· radicals polymerizing into a singlet state oligomer. White spheres, H; gray, C; red, O; yellow, S; blue, N; purple, I^-. Reprinted with permission from ref. 14. Copyright © 2014 John Wiley and Sons.

Finally, the oxidation reactions that are illustrated in **Figure 7**a and b formed the DME(H^-) radicals in **Figure 7**c. These radicals would readily undergo exothermic (-258 kJ/mol) condensation reactions and form linear or comb-branched oligoethers. These formed oligoethers (i.e. polymerization) would result in the formation of the protective film that was observed via SEM on the Li-metal anode and sulphur cathode (**Figure 8**a and b).[14]

Via SEM, the Li-metal anode (**Figure 8**a) and sulphur cathode (**Figure 8**b) are shown to have a smooth polymer-like film on the surface after 100 cycles. Furthermore, the Li-metal anode surface (**Figure 8**a) exhibits no visible dendrites nor Li_2S particles visible after the cycling.

Furthermore, the SEM analysis discovered a net-like porous structure (**Figure 8**a) of the Li-metal SEI. This might improve the anode's ability to diffuse ions more rapidly and readily.[14]

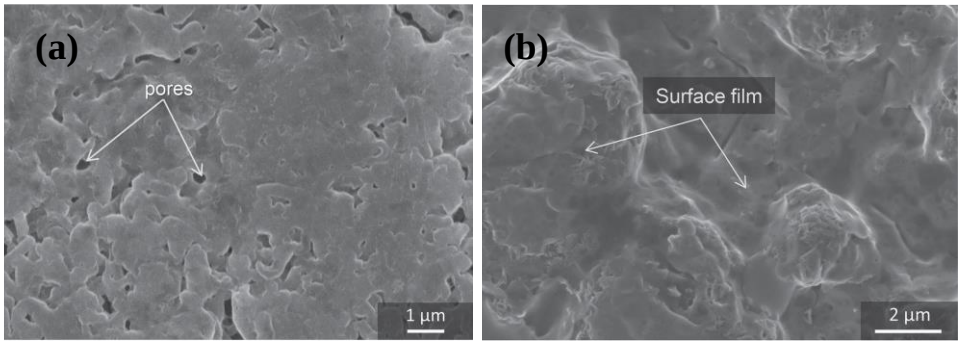

Figure 8: SEM of a) Li-metal anode and b) sulphur cathode after 100 cycles in an electrolyte containing LiTFSI (5M) and LiI (0.5M). Reprinted with permission from ref. 14. Copyright © 2014 John Wiley and Sons.

1.5 XPS (X-ray photoelectron spectroscopy)

Photoelectron spectroscopy is based on the photoelectric effect, where a sample is illuminated with a beam of photons with an energy that is defined to be greater than the ionization energy required to emit electrons from the sample.[17] There are different types of photon sources available for laboratory-based setups, e.g., X-ray tubes. Their anodes commonly consist of Mg or Al, with photon energies of 1253.6 and 1486.6 eV, respectively. Singe crystal X-ray monochromators that are coupled to Al anodes can significantly improve the energy resolution to <0.3 eV. Furthermore, the monochromator filters away the satellite emission peaks.[19]

1.5.1 Sample preparation

Photoelectron spectroscopy is a technique that is highly surface sensitive, which can gather information of samples at depths of only a few nanometers. The photoemission experiments usually take place in ultra-high vacuum ($<10^{-7}$ Pa). This ultra-high vacuum must be maintained in order for electrons to reach the detector without collision with atmospheric molecules (such as O_2, N_2, CO_2 and etc.) or else unaccounted energy loss will occur to the electrons emitted from the sample.[19]

1.5.2 XPS analysis of SEIs

Interphases that are buried beneath the top surface can be important for a large number of devices, such as batteries. The high surface sensitivity of XPS prevents one to be able to analyze chemical and electronic properties of interfaces that are buried beneath deposited layers. The deposited layer's thickness will determine whether the layers beneath can be detected. In this

work, the layer of interest is the deposited layer. However, one can overcome this restriction by analyzing the surface at different deposition times.[19] In this thesis the Li-metal is immersed in electrolytes for different time durations. Therefore, it is possible to observe the chemical species of the SEI, layer by layer.

1.5.3 Elemental and composition analysis

An important step to evaluate which elements are present at the sample's surface is to run a survey spectrum, which spans from 0-1487 eV.[19] Each core level of an element has characteristic binding energy (BE) values. The *Handbook of X-ray Photoelectron Spectroscopy* is a useful reference to identify peaks.[18]

XPS is one of the most effective techniques to analyze the chemical composition of a surface. Furthermore, in some cases it is possible to perform quantitative analysis with XPS. Although, many factors can contribute in how the peak intensities are obtained, such as inhomogeneous surfaces.[19]

The first step in a surface compositional analysis would be to extract the peak intensities, which would start with doing a background subtraction. Linear or polynomial functions are used to fit the inelastic background, using methods such as Shirley[21] and Tougaard[22], which are simply physical approaches. Shirley's prediction states that a certain amount of primary electrons are lost inelastically, which are proportional to the number of integral photoelectrons excited. That would make the inelastic background function proportional to the integral of the whole photoelectron spectrum, which would start from kinetic energies with the highest values at the Fermi energy level.

Curve fitting would have to be performed if the intensities of different chemical species of an element are to be assessed, especially if the peaks overlap. For chemical species that are non-metallic, the peaks are usually symmetric and therefore the fittings are reproduced by a convolution of Gaussian and Lorentzian curves.[23]

2 Aim and objectives

The introduction reviewed various methods to improve SEI's and prevent dendrite formation on Li-metal anodes. However, the resources and time available only allow an investigation to a certain extent. The main goal was to investigate how LiI as an electrolyte additive affects the SEI of Li-metal. This was done along with other electrolyte salts (LiTFSI) and additives ($LiNO_3$ and LiBOB). It has been reported that LiI induces the formation of stable polymers on Li-metal that improves cell performance, as explained in section 1.4.2. The components will be explained in detail in the *Experimental procedure* section. This project will be carried out by performing XPS measurements to investigate the chemical species of the SEI. This could reveal whether any of the expected and/or unexpected reactions are taking place on the Li-metal surface. SEM analysis will be performed to obtain a clearer picture of the morphology of the Li-metal anodes. The electrochemistry, for this type of Li-metal battery, has been investigated quite thoroughly in a few publications[14,44], but little has been reported on its surface chemistry with XPS. Therefore, this thesis will focus on performing systematic studies of the Li-metal surface at different additive concentrations and time durations in contact with the electrolytes.

3. Experimental procedure

3.1 Preparation of salts and solvents

The following salts were components of electrolyte solutions in this work: Lithium nitrate ($LiNO_3$, (Alfa Aesar, anhydrous 99%)), LiTFSI, (BASF), LiI (lithium iodide (Alfa Aesar 98+ %)), LiBOB (lithium bis(oxalato)borate, (Chemtail)). The solvents that were used were dimethyl carbonate (DMC, Sigma Aldrich, anhydrous ≥99%), propylene carbonate (PC, Gotion), 1,3-dioxolane (DOL, Sigma Aldrich, anhydrous 99.8%), dimethoxyethane (DME, BASF). The previously mentioned Li-salts were dried in a Büchi oven under vacuum, inside a glovebox filled with argon atmosphere according to a reference assigned to each one of them. This was done to get rid of any trace amounts of H_2O which would deteriorate the Li-metal anode. The O_2 (1-10 ppm) and H_2O levels (1-10 ppm) were low in the powder glovebox. However, according to the logbook when the experiments were carried out, it was reported that the O_2 and H_2O levels reached up to 50 and 130 ppm respectively. This was usually for a short amount of time and usually happened when the glovebox was being regenerated. However, this could have affected the samples. Even though they were properly sealed, the O_2 and H_2O could have diffused into the samples.

The $LiNO_3$ was dried at 120 °C overnight (c.a 18 hours)[24], LiTFSI at 120 °C overnight as well[25], LiI at 160 °C overnight (160 °C needed in case $LiI{\cdot}3H_2O$ was present, which needs at least 130 °C to become anhydrous)[26], LiBOB was dried at 120 °C overnight[27]. The solvents were dried in molecular sieves (Merck 0.3 nm (~2 mm/ ~10 mesh)). The molecular sieves were activated in a vacuum oven at ~200 °C overnight (12-18 hours).

3.2 Preparation of electrolytes

The electrolytes were prepared in a different glovebox (assembly glovebox), in order to reduce the risk of contaminations of solid materials. The O_2 (1-10 ppm) and H_2O levels (1-20 ppm) were not as consistent in the assembly glovebox as the powder glovebox, over the period when the electrolytes were prepared. According to the logbook over the period when the experiments were performed, the O_2 and H_2O levels reached up to 250 ppm.

To simplify the concentration of the electrolytes, the volume of the salts/additives were not taken into account of the molarity. Instead, molality (M) was used, which is moles (n) of salt per gram of solvent (m), as depicted in equation 2.

$$1\ \mathrm{M} = \frac{\boldsymbol{n}}{\boldsymbol{m}} = \frac{0.01\ \mathrm{moles}}{10\ \mathrm{g}} \tag{2}$$

The solvents were filtered with syringe filters (VMR (25mm diameter; 0.2 µm; polypropylene membrane)) before added to weighed salt components. This was done to avoid Si contaminations (from the molecular sieves). Once the salt components had been stirred in the solvent overnight, they were filtered once again since dust contamination from the salts were visible in the prepared electrolyte. Note that double filtering is necessary, since after stirring an unfiltered solvent with the salts, it is possible that the molecular sieve particles become small enough to pass through the polypropylene membrane.

The solvents that were used further on, for Li-metal dipping was pure DMC, PC, DOL and DME. For electrolytes, DOL and DME solvent mixture of 1:1 weight ratio was used for all electrolyte experiments. This 1:1 by weight ratio was obtained by weighing each solvent dropwise on a scale. All prepared electrolytes were kept consistently at the amount of 3.00 grams of solvent. The concentrations of each electrolyte component are depicted in **Table 1**.

Table 1: Concentrations of electrolytes in DOL:DME (1:1 by w.)

[LiTFSI] (M)	[$LiNO_3$] (M)	[LiBOB] (M)	[LiI] (M)
1.000	0.250		
1.000	0.250		0.100
1.000	0.250		0.200
1.000	0.250		0.500
1.000		0.200	
1.000		0.200	0.100
1.000		0.200	0.200
1.000		0.200	0.500

Furthermore, glass vials had to be used. Since the electrolyte solvent appears to be corrosive against aluminum, therefore those type of vials could not be used for experimentation, see **Figure 9**. The electrolyte being corrosive towards aluminum could cause problems if one were to assemble a battery, since one of the current collectors consists of aluminum.

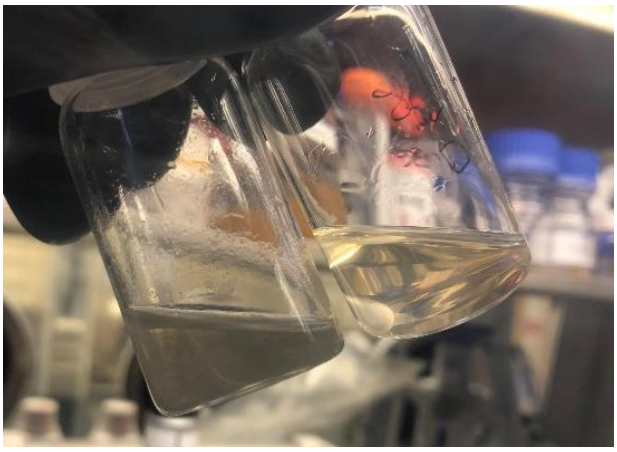

Figure 9: Electrolytes containing LiTFSI (1M); $LiNO_3$ (0.25M) and LiI (0.50M), after being in an aluminum vial (on left) and glass vial (on right) for approximately 2 weeks.

3.3 Li-metal dipping in electrolyte experiments

The electrolytes were transferred from one glove box to another, since the electrolytes must be prepared in a different glovebox (powder glovebox) to minimize unaccounted contamination against the electrode materials, which are in the assembly glovebox. Therefore, the electrolyte solutions were transferred to the assembly glovebox via a sealed transfer vial, to give an extra layer of protection from atmospheric air.

In the assembly Ar-filled glovebox, Li-foil was cut into appropriately sized (circa 15x7 mm) rectangles (**Figure 10**), placed into solvents/electrolytes and left for a fixed time duration ranging from 30 minutes to approximately 4 months, since the goal was to analyze the samples at fixed durations. The Li-metal foils were not pretreated in any way, such as brushing or chemical cleaning. It was important for the Li-foil to be in contact with the solution during the whole time of the experiment, in order to obtain consistent results.

3.4 Preparation of samples for XPS and SEM analysis

Before XPS or SEM analysis can take place, the Li-metal foil must be washed. This is done to minimize the amount of electrolyte residue sticking to the Li-metal surface, since the main objective is to investigate the SEI formation. This is done by carefully dripping a few drops of a blank solution, containing only DME:DOL (1:1 by w.) and no Li-salts. For best results, the Li-foil should be held vertically during the washing, this will give a more even wash, making the chemistry on the surface more likely to be uniform. The edge of the foil is then placed gently against a paper towel, which soaked up most of the solvent. Followed with leaving the foil on a pristine clean surface to dry for a few minutes before placing it on a double-sided conducting copper adhesive tape (**Figure 10**). It was important to let the side that had not touched any

surface, to face upwards on the XPS sample holder. There is always the possibility of contamination or destruction of the SEI from touching or scratching a surface.

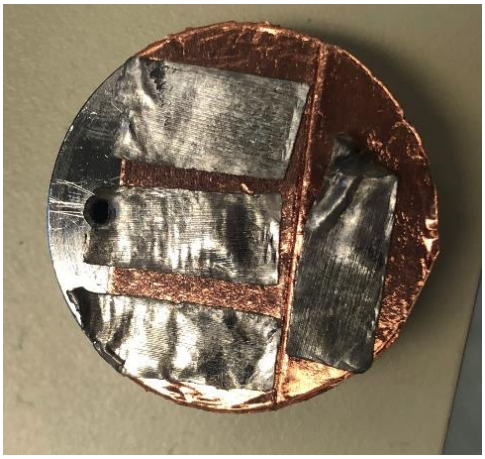

Figure 10: Li-metal foils, after being dipped in electrolyte for 4 months placed on a copper adhesive sample holder before being transferred for XPS analysis.

Multiple Li-metal foils were added to the electrolyte samples simultaneously. This was only done once for each electrolyte sample. Fresh electrolytes were prepared for each experiment. Extraction of the Li-metal foils were done at different time durations, to be analyzed via XPS.

3.5 XPS analysis

The sample holder was transferred to the XPS via a transfer cup, to prevent the samples from reacting with the atmosphere. The XPS (Perkin Elmer PHI 5500 system) is equipped with an Al-anode which emits X-rays (1486.7 eV). Once the sample is in the main chamber, which operates under ultra-high vacuum conditions, an alignment of the sample must take place, in order to achieve maximum signal intensity. This is important to do properly and consistently, otherwise the spectra will not be normalized against each other. This is done by doing a manual alignment (moving the sample up and down) and compare the signal intensity on *Augerscan 3*. Depending on the elements present on your sample and their quantity, the element that gives the strongest signal should be used to tune the alignment. For a pristine Li-metal it would typically be O 1s or C 1s, but for the samples in this thesis it was either F 1s or O 1s.

Once maximum signal was achieved, a survey scan was carried out. This obtained the whole spectrum of elements. From the survey, it is important to pinpoint all the elements of interest and run single scans of those chosen elements. This will project higher resolution spectra, which will reveal the peaks of interest for further scans (multiplex). Furthermore, it is important to scan 4 eV extra on both sides of the peaks for background. This is necessary for reliable peak fitting, which is discussed in greater details in section 3.4. Before proceeding with a time-

consuming multiplex analysis, it is recommended to analyze different areas of the sample with single C 1s scans. This is done to make sure that the Li-metal surface is uniform. If not, one should find an area, which exhibits the most common peak pattern throughout the sample. If necessary, one should repeat that sample by retrieving a fresh Li-metal foil from the electrolyte and do the whole process again (cleaning, drying and etc.). A rule of thumb, the higher the intensity of the peak(s), the fewer the scans required to obtain a higher resolution spectra. The parameters for alignment, survey and multiplex are depicted in **Table 2**. The table exhibits different values of eV/step (resolution), pass energy and time/step (amount of time measured at each interval).

Table 2: Operational parameters for XPS experiments regarding alignments, surveys and multiplexes.

	Alignment	Survey	Multiplex
eV/step (eV)	0.400	0.400	0.100
Pass energy (eV)	187.85	187.85	23.50
Time step (ms)	20	200	200

3.6 Fitting XPS data

The obtained raw data from *Augerscan 3* is transferred to another software, *CASA XPS*, for data analysis. This software is designed to add peak fittings to the spectra. First of all an applicable background type must be used. The Shirley background is useful when overlapping peaks with different scattering factors are present.[28] Therefore, Shirley was used for all spectra in this thesis. For C 1s and O 1s fitting, GL(30) is most commonly used.[29] GL(30) consists of 70% Gaussian and 30% Lorentzian.

4. Results and Discussion

4.1 XPS analysis of Li-metal dipping in various solvents

Li-metal foil was immersed in various solvents (**Figure 11)** for fixed time durations. The XPS analysis obtained the chemical species on the Li-surface which were identified according to reliable sources, as depicted in **Table 3**.[30] The C 1s XPS of DME and DOL (**Figure 12**a and b) individually look identical. The DME molecule (**Figure 11**a) does not have an O-C-O species, which DOL has (**Figure 11**b). Therefore, one could assume that the O-C-O peak (~288.2 eV) for DME (**Figure12**a) is a contamination. The DME and DOL sample were prepared at the same time in the glovebox. It is possible that the fumes of the solvents cross contaminated with the Li-metal foils while they were being placed on the XPS sample holder. Another possibility is that the O-C-O species was there before the Li-metal foil was immersed in the solvent (**Figure 12**f).

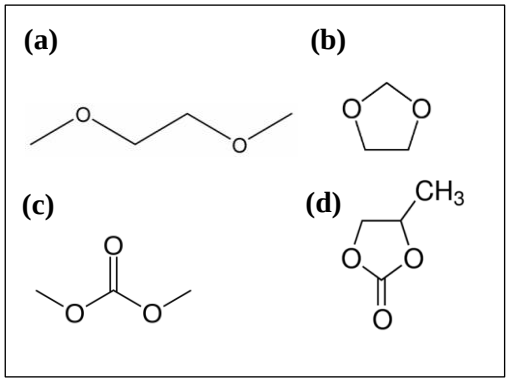

Figure 11: Chemical structures of the solvents used for Li-metal foil dipping. a) DME; b) DOL; c) DMC; d) PC

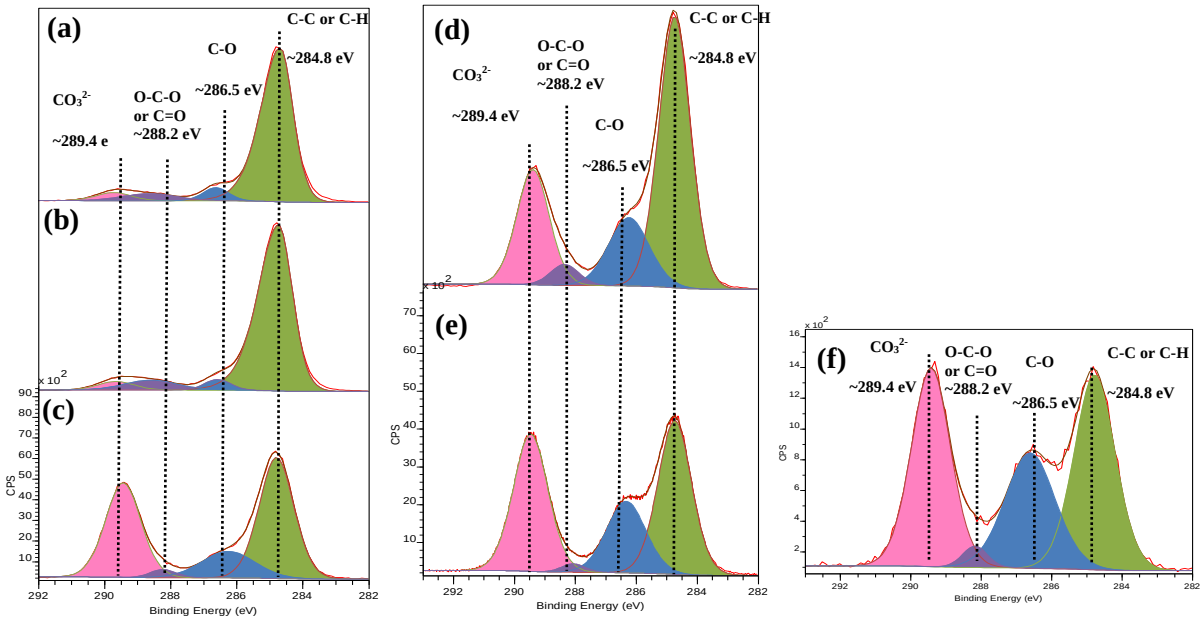

Figure 12: C 1s XPS spectra's of Li-metal foil dipped in the following solvents: a) DME (30 min); b) DOL (30 min); c) DOL:DME (4 days) (1:1 by w.); d) DMC (4 days); e) PC (2 days); f) Pristine Li-metal foil. Peaks are depicted in table 3.

Calibrations of spectra in **Figure 12** were optimized in terms of the C-C/C-H peak. It was assumed to be at 284.8 eV.[30,32] The peaks exhibiting at ~289.5 eV (in pink) in all the spectra in

Figure 12, are characteristic for CO_3^{2-} species (most likely a carbonaceous salt, f.ex. Li_2CO_3).[30] Various conclusions can be drawn from the low intensity of the CO_3^{2-} peaks for DME and DOL (**Figure 12**a & b), relative to the DME:DOL and pristine Li-metal spectra (**Figure 12**c & f). It is possible that there was a cross contamination for the DME:DOL (**Figure 12**c) and DMC sample (**Figure 12**d) as well. These two samples were prepared at the same time in the glovebox. Contamination from DMC is a possibility, since the CO_3^{2-} peak (~289.5 eV) is much more intense for the DOL:DME sample (**Figure 12**c) compared to the individual ones (**Figure 12**a & b).

The pristine Li-metal foil (**Figure 12**f) exhibits carbon species that are likely to be contaminants from solvents that are commonly used for cleaning in the assembly glovebox, such as DMC and methanol. In order to draw more conclusions of how the solvents alone are reacting with the Li-metal, more data would be required, such as dipping for different time durations.

4.2 XPS analysis of Li-metal in LiTFSI and $LiNO_3$ based electrolytes

Polymerization of DME molecules was discussed in section 1.4.2, which is involved with the presence of LiI. The QC studies suggest that this polymerization process involves C-C bonds forming between DME molecules, as **Figure 7**c depicts.[14] Therefore, it is assumed that the amount of carbon atoms in the C-C electronic state will increase as the polymeric chain gets longer. In a single DME molecule (**Figure 10**a) there are two equivalent C atoms ($H_3\underline{C}$-O) in the terminals and two equivalent C atoms (C-$\underline{C}$-O) in the center of the molecule. Therefore, the hypothesis is that the ratio between the C-C (green peaks on far right, **Figure 13**) and the C-O peak (blue, **Figure 13**) shift more towards the C-C electronic state as more LiI is added.

After 2 hours, **Figure 13**a, the abovementioned trend is not apparent. It is not until after 72 hours when a trend could be detected (C-C:C-O ratio, as depicted next to those peaks on **Figure 13**). The C-C:C-O ratio increases from 0 – 500 mM LiI (**Figure 13**c i-iv), if the 200 mM LiI sample (**Figure 13**c iii) is excluded. The rest of the spectra in **Figure 13** exhibit a lack of consistency in terms of the C-C:C-O ratio. As mentioned before, the samples revealed to be quite inhomogeneous at the Li-metal surface. The spots that were measured had to be chosen carefully. This was done by carrying out quick single scans (C 1s preferably) at multiple locations across the Li-metal surface. The most common and distinctive pattern was chosen for higher resolution analysis. On the other hand, what could have been done instead was to combine all the spectra from different locations to obtain an average spectrum. This would however, be extremely time consuming.

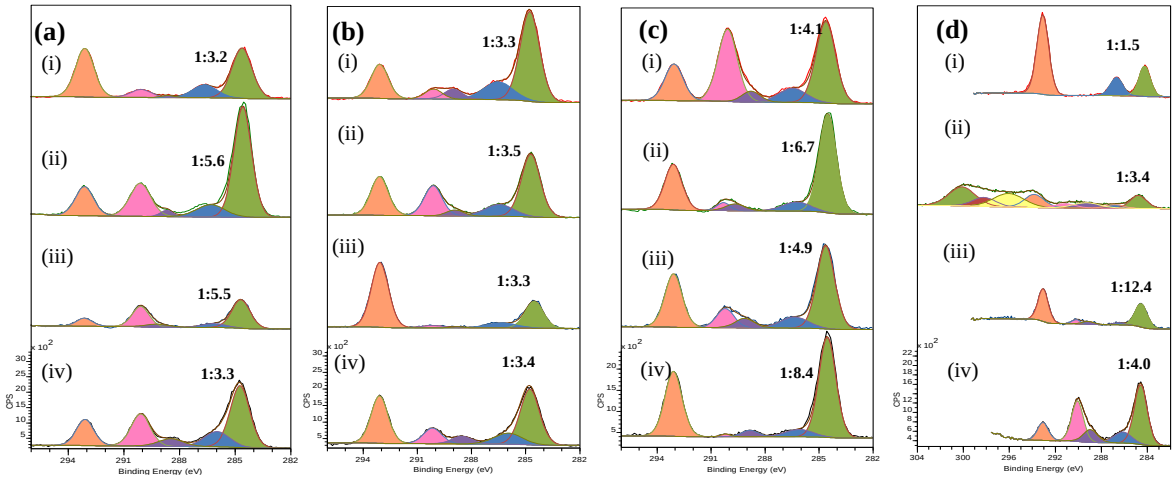

Figure 13: C 1s XPS spectra of Li-metal dipped in electrolyte for a.) 2h b.) 24h c.) 72h d.) 20 days. Electrolyte contained 1.0 M LiTFSI, 0.25 M $LiNO_3$ in DOL:DME (1:1 by w.). i.) No LiI. ii.) 100 mM LiI. iii.) 200 mM LiI and iv.) 500 mM LiI. Peaks are depicted in table 3.

Table 3: XPS binding energies with attributed species and their assumed origin.

Element spectra	Binding energy (eV)	Colour	Species	Ref.	Assumed origin
C 1s	284.8	Green	C-C/C-H	30	DOL/DME residue and/or DME oligomers
	286.5	Blue	C-O		DOL/DME residue or decomposition products or polymeric species of carbonyl
	288.2	Purple	O-C-O		DOL decomposition products
	289.4	Pink	Li_2CO_3		Lithium carbonates and/or semicarbonates
	293.1	Orange	$–CF_3$		LiTFSI
	296.0 298.2 300.1	Yellow, red and green (far left)	CF_xI_y and/or $(CF_2\text{-}CF_2)n$	33,36	LiTFSI decomposition products or charging effect
F 1s	689.6	Green	$\text{-}CF_3$	30	LiTFSI
	691.0 693.2 694.8	Blue Purple Pink	CF_xI_y and/or carbonfluroide polymers	33	LiTFSI and/or DOL/DME and/or LiI decomposition products
	685.8	Orange	LiF	30	Decomposition product from LiTFSI
N 1s	399.9	Green	$Li\text{-}N(SO_2\text{-}CF_3)_2$	30	LiTFSI
	400.7	Blue	Unknown		Assumably a LiTFSI decomposition product or from charging effect
	403.4	Purple	$LiNO_2$	38	$LiNO_3$ or a LiTFSI decomposition product
	407.8	Yellow	$LiNO_3$	34	$LiNO_3$
I $3d_{5/2}$	619.1	Green	LiI or I_2 (elemental iodine)		LiI and/or decomposition product of LiI, such as elemental iodine (I_2)
	621.4	Blue	CF_xI_y or CH_xI_y	33	LiI decomposition products
	623.2	Purple	I_2O_5	29, 39	LiI decomposition products
	624.9	Pink	$LiIO_3$	40	LiI decomposition products

The CO_3^{2-} peaks (in pink, 289.4 eV) in **Figure 13**c (after 72 hours) decrease in intensity as more LiI is added to the electrolyte. This pattern could indicate that something is gradually forming (**Figure 13**c) on top of the Li_2CO_3.

The 100 mM LiI sample (ii) on **Figure 13**d exhibited an unusual cluster of C 1s peaks. The BE of these peaks are rather high, with values of 296.0; 298.2; 300.1 eV (as depicted in **Table 3**). These peaks could be due to static charge from the $–CF_3$ groups of LiTFSI residue on the surface. Due to the porous nature of lithium, it might be difficult to rinse out all salt residues that are clogged up in the pores. Hydrocarbons, carbon oxides and carbon fluorides could exhibit poor electrical conductivity. These species could acquire positive charge during experiments, which would lead to shifts towards higher BE.[32] Hypothetically, if these higher BE peaks in **Figure 13**d are not due to charging, it is possible that they are a complex polymeric chain of $(CF_3[(\text{-}OCF(CF_3)C\text{-}F_2)_n(\text{-}OC\text{-}F_2)_m]_xOCF_3)_n$ like species, according to the C 1s (**Figure 13**d (ii)) spectra.[33,36] Polymeric chains could be a result of decomposition of LiTFSI, the solvent and/or iodine. If these high BE peaks are not due to a charging effect, they will be difficult to characterize. There is a lack of publications related to these binding energy values.

Other lithium halides, such as LiF, LiCl and LiBr follow a trend in BE on Li 1s, 55.6; 56.0; 56.8 eV. Therefore, one could assume LiI appears at >56.8 eV. However, LiI could not be detected on the Li 1s spectra (**Figure S1**). It is very difficult to draw conclusions from the Li 1s spectra. The signal to noise (S/N) ratio is too low to perform accurate peak fitting.

An indication of CF_xI_y or CH_xI_y species would be by taking a closer look at the F 1s and I $3d_{5/2}$ spectra (**Figure 14**a & c). Iodine exhibits a spin orbital split (doublet), but to simplify, only the peaks at the lower binding energy region are shown (**Figure 14**c), since their peaks are more intense. The doublet appears because iodine has two spin states in the 3d orbital (5/2 and 3/2). The green peak (619.4 eV) in the I $3d_{5/2}$ spectra (**Figure 14**c) would represent LiI or elemental iodine (I_2).[18] It is reported that when iodine is bound to carbon, it appears at ~621 eV on XPS.[33] Therefore, based on the information available, there could be at least one iodine species bonded to carbon (Blue peak, 621.4 eV, **Figure 14**c), which could be a hydrocarbon, such as from either of the solvents or the $\text{-}CF_3$ carbon on LiTFSI. The other two peaks (purple and pink) on the I $3d_{5/2}$ spectra (**Figure 14**c) could be from I_2O_5 (623.2 eV)[39] and $LiIO_3$ (624.9 eV)[40] species. However, when LiI is exposed to air, it turns yellow. This is due to the oxidation of iodide to

iodine, according to equation 2:[41, 42] However, the LiI used was slightly yellow, therefore likely to have been exposed to O_2 at some point. Pure LiI is a white solid.

$$10LiI + 5O_2 \leftrightarrow 4I_2 + 4Li_2O + 2LiIO_3 \quad (2)$$

According to a publication[43], DME solvent in presence of iodine (I_2), could oxidize Li_2O_2 (equation 3). The produced I^- could then form I_3^- with the remaining I_2 (equation 4). $LiIO_3$ is known to have formed in the presence of LiOH, which forms in the presence of cells being discharged with LiI in DME and I_3^- (equation 4). Therefore, the formation of $LiIO_3$ could come from equation 5.

$$I_2 + Li_2O_2 \rightarrow 2Li + 2I^- + O_2 \quad (3)$$

$$I_2 + I^- \leftrightarrow I_3^- \quad (4)$$

$$3I_3^- + 6LiOH \rightarrow 2I^- + 2Li^+ + H_2O + LiIO_3 \quad (5)$$

It is possible that LiOH is present in the electrolyte and SEI of the Li-metal, since a white precipitate was in the electrolyte after circa 2-3 weeks of dipping, both for the $LiNO_3$ and LiBOB experiments. An attempt was made to filter the white precipitate from the 500 mM LiI samples, which was unsuccessful due to the amount was too little. The precipitate was only visible in the electrolytes containing LiI. Therefore, one can assume LiI plays a role in its formation.

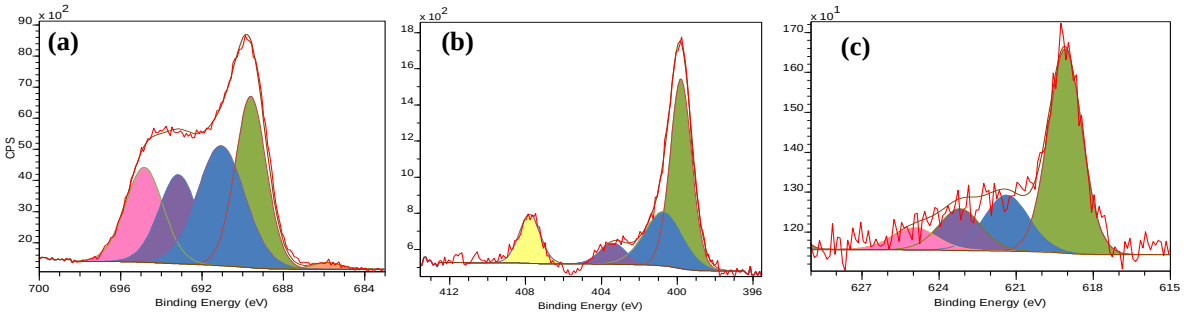

Figure 14: XPS spectra of Li-metal dipped in electrolyte for 20 days. a) F 1s b) N 1s c) I 3d5/2. Electrolyte contained 1.0 M LiTFSI, 0.25 M LiNO3 and 100 mM LiI in DOL:DME (1:1 by w.). Peaks are depicted in table 3.

However, it is difficult to confirm its presence with XPS, since the LiOH (54.9 eV) peak on Li 1s (**Figure S1**) would be at approximately the same binding energy as Li-metal (55.0 eV).[18] Furthermore, the S/N ratio is rather low for Li 1s (**Figure S1**), which makes peak fitting of the Li 1S less reliable. Calibration of all the spectra in this section (4.2) was done in terms of the CF_3 peak of LiTFSI.[30, 31]

$LiNO_3$ appears at 407.8 eV[37,38] on N 1s (**Figure 14**b), its decomposition species such as RCH_2NO_2 (393.7 eV)[37]; R-O(LiN_xO_y) (395.6 eV)[37]; Li_3N (398.5 eV)[37]; $Li_2N_2O_2$ (399.3 eV)[37], did not appear on any of the samples on N 1s. The purple peak on **Figure 14**b, could be $LiNO_2$ (403.4 eV)[38]. Interestingly, this peak only appeared in samples that contained LiI. Therefore, one can assume that these peaks are associated with the presence of LiI. The same applies for the blue peak at 400.7 eV (**Figure 14b**). However, the blue peak in **Figure 14**b does not match with any of the reported decomposition products of $LiNO_3$ nor LiTFSI.[30, 31, 37, 38] Therefore, an assumption can be made that it is from a charging effect of LiTFSI. Furthermore, no N 1s peaks appeared on the pristine Li-metal. Therefore, pre-deposited contamination can be ruled out.

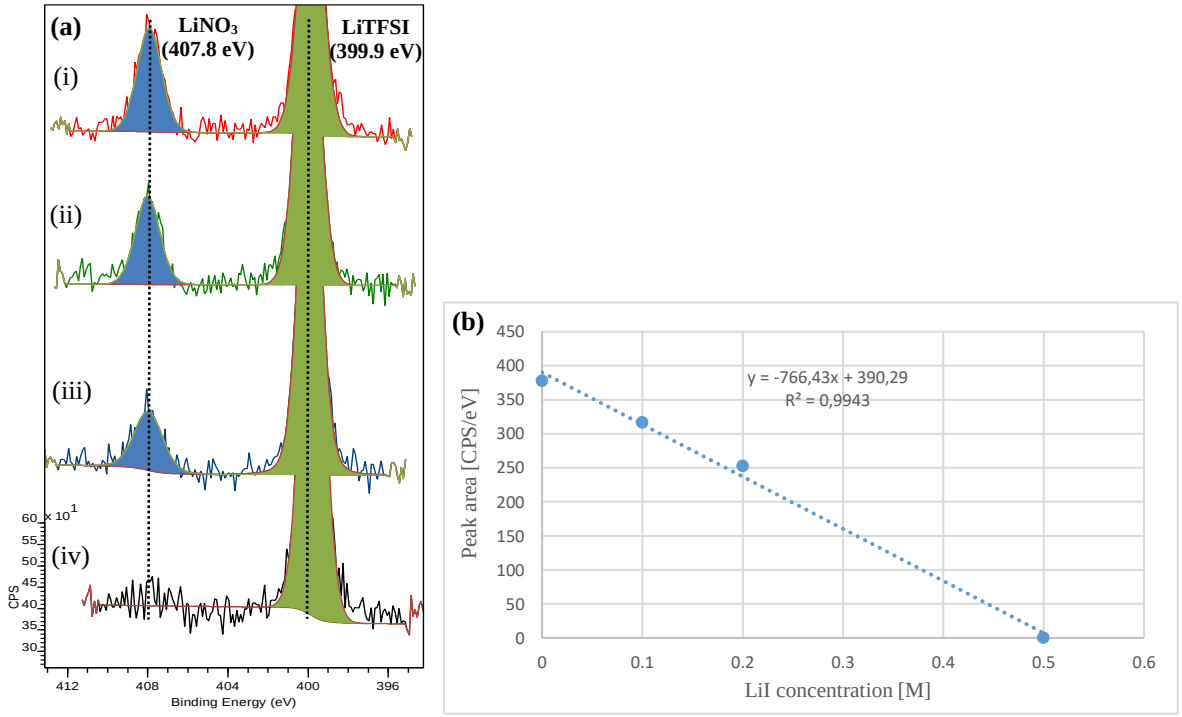

Figure 15: N 1s XPS spectra of Li-metal immersed in electrolyte for 72 hours. a) (i)No LiI; (ii) 100 mM; (iii) 200 mM; (iv) 500 mM LiI. b) Peak area of $LiNO_3$ peaks plotted against different concentrations of LiI. Electrolyte contained 1.0 M LiTFSI, 0.25 M $LiNO_3$ and various concentrations of LiI in DOL:DME (1:1 by w.). Peaks are depicted in table 3.

The N 1s spectra (**Figure 15**a) after 72 hours of immersing in electrolyte revealed a trend, similar to the CO_3^{2-} peaks (in pink, 289.5 eV) in **Figure 13**c. The $LiNO_3$ (407.8 eV) peaks in **Figure 15**a (i-iv) decrease in intensity as more LiI is added. This gradual decrease is clearer in **Figure 15**b, where the peak area of $LiNO_3$ is plotted against the concentration of LiI. There is clearly a linear connection between these two. This could indicate that LiI is involved with forming an organic a layer on top of the $LiNO_3$ in the SEI. Furthermore, another conclusion

could be made. The LiI prevents the $LiNO_3$ additive from forming on the Li-metal surface. This means that LiI could be used to control how much $LiNO_3$ forms on the Li-metal surface.

4.3 XPS analysis of Li-metal in LiTFSI and LiBOB based electrolytes

In this section, another additive was studied. This was done by performing the experiments with same procedure as in section 4.2, except $LiNO_3$ was substituted for LiBOB. It has been reported that LiBOB is a potential candidate to be used in Li-ion battery systems. In a publication,[35] it exhibited improved (electrochemical) results when used with LiTFSI in a Li-S battery system, in contrast with not using LiBOB. The optimal concentration of LiBOB was 4 wt%, which corresponds to approximately 0.20 M. Its advantages are that it is more thermally stable than $LiNO_3$, less pollutant since its decomposition products are not as toxic and corrosive. Furthermore, it is able to form stable SEI films on graphite electrodes.[35] Herein, it was studied with Li-metal anodes.

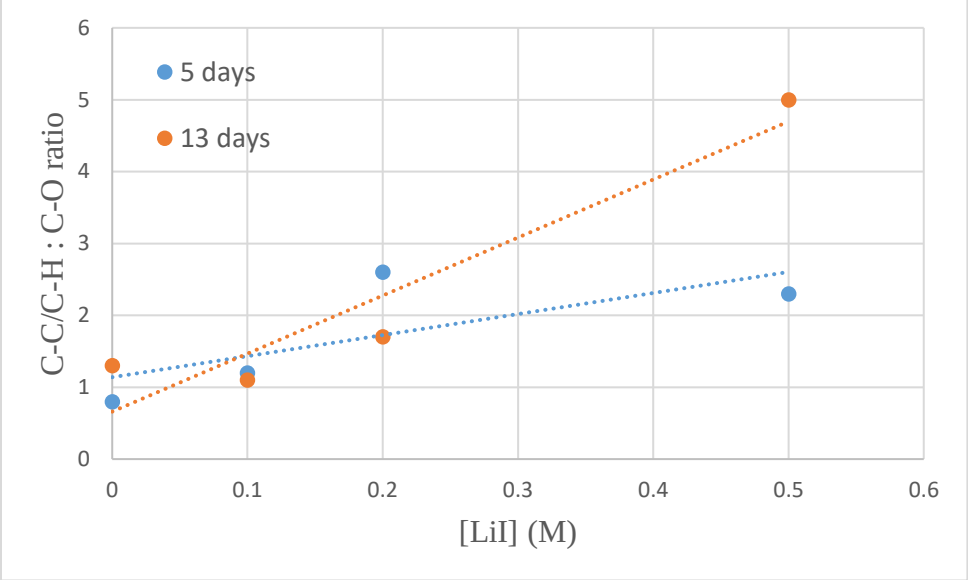

Figure 16: Comparison of relative peak intensity of C-C/C-H (~284.8 eV) and C-O (~286.5 eV) species vs. fixed LiI concentration. Blue series: 5 days of Li-foil dipping; Orange series: 13 days of dipping.

The Li-metal was immersed in the electrolyte for 5 days with different concentrations of LiI, which showed a consistent trend in terms of the C-C:C-O ratio. The C-C:C-O ratio (**Figure 16**) increases as more LiI is added to the electrolyte. It is difficult to predict a mechanism based on this data. According to literature[14], the DME is mostly involved with the polymerization (**Figure 7**). However, DOL tends to react with the Li-metal itself to form various decomposition products (**Figure 17**).[1] Furthermore, the $–CF_3$ (orange peak) and CO_3^{2-} (pink) peaks decrease

in relative intensity as more LiI is added, after 5 days and 13 days of dipping (**Figure 20**a & b). This is a strong indication for a SEI formation, seen in **Figure 13**c as well.

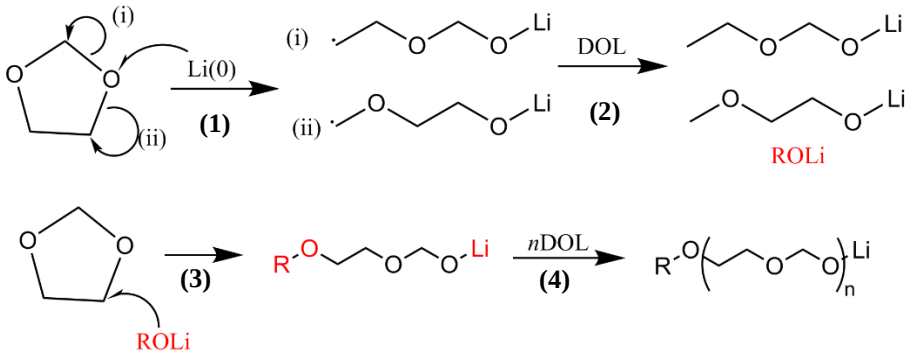

Figure 17: Proposed mechanism of DOL solvent undergoing surface reaction with Li-metal to form DOL based polymers. Image based on ref. 1 with modifications.

D. Aurbach et al. reported that DOL reacts with Li-metal to form a polymer product (**Figure 17).**[1] A ring opening takes place (1) when the uncharged Li(0) reacts with the oxygen of DOL. Different (i or ii) hydride aliphatic intermediates are formed. The radicals abstract a hydrogen from DOL (2), to form stable ROLi. The ROLi reacts with a DOL molecule (3), resulting in a longer chain of ROLi. Step (4) is a repeat of step (3) to form DOL polymers.

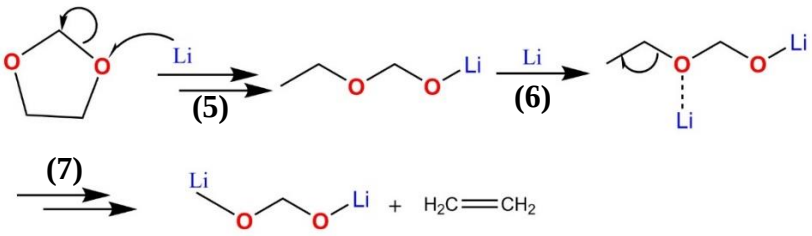

Figure 18: Proposed mechanism of DOL solvent undergoing surface reaction with Li-metal to form Li-O-C-O-Li and ethylene products. Image based on ref. 53 with modifications.

Another proposal of how DOL reacts with the Li-metal surface was published by X. Chen et al.[53] The DOL does not form a polymer, but instead Li bonds with the two oxygens of DOL and forms ethylene gas (**Figure 18**). The DOL molecule undergoes a ring opening (5) from the Li reacting with one of the oxygens. Li reacts with the other oxygen (6), which eliminates an ethylene group (7).

The proposed mechanism for DME with lithium (**Figure 19**) is also published by X. Chen et al.[53] After Li has reacted with one of the oxygens (8), a CH_3OLi group breaks away (9), as

depicted in **Figure 19**a. The hydride (H^-) radical forms another CH_3OLi group, along with ethylene gas. (10-11).

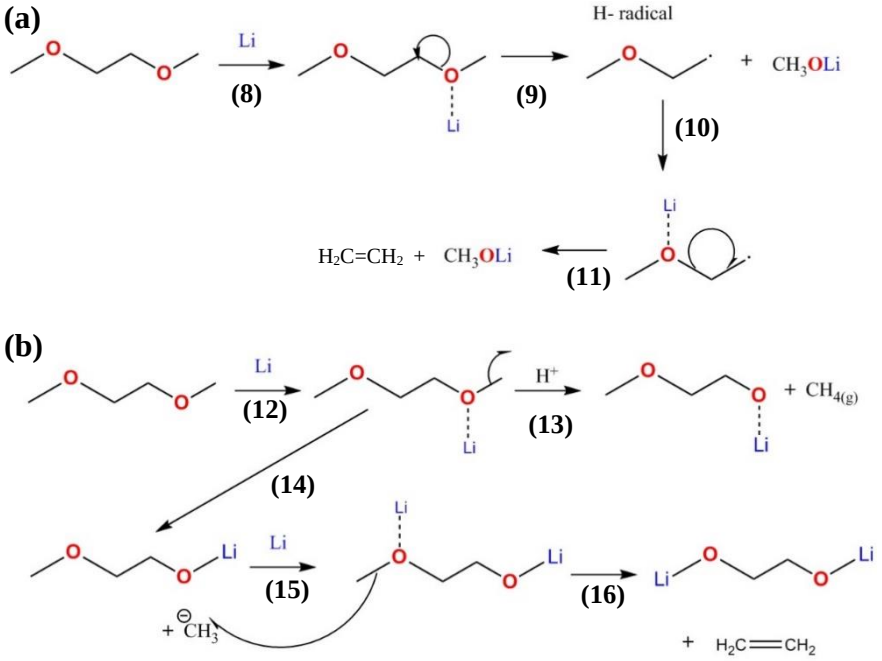

Figure 19: Proposed mechanism of DME solvent undergoing surface reaction with Li-metal to form a) Li-O-CH_3. b) Li-O-R-O-Li, methane and ethylene products. Image based on ref. 53 with modifications.

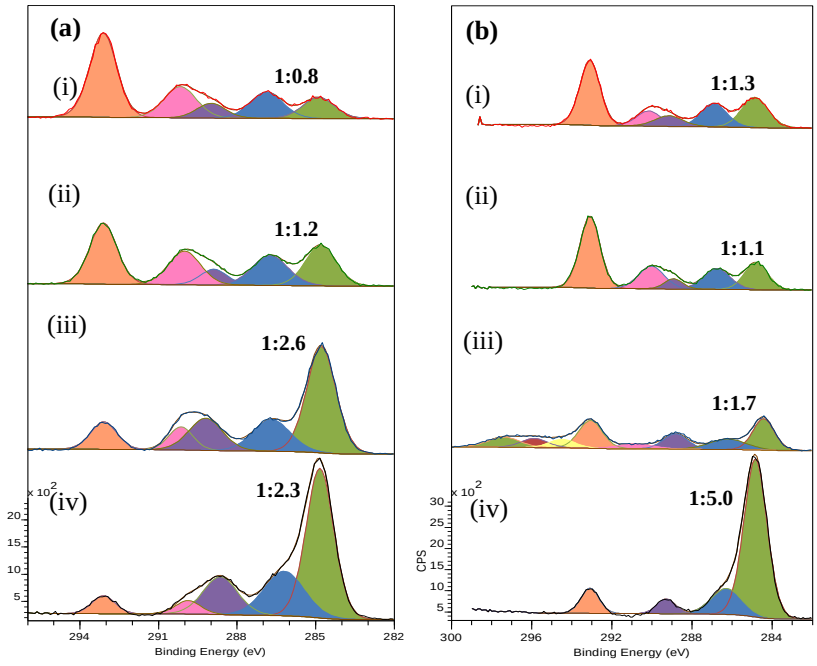

Figure 20: C 1s XPS spectra of Li-metal dipped in electrolyte for a.) 5 days and b.) 13 days. Electrolyte contained 1.0 M LiTFSI, 0.20 M LiBOB in DOL:DME (1:1 by w). i.) No LiI. ii.) 100 mM LiI. iii.) 200 mM LiI and iv.) 500 mM LiI. Peaks are depicted in table 3.

Another proposal of DME reacting with Li, could result in the formation of methane (13), as depicted in **Figure 19**b. The terminal methyl groups could also be the leaving groups, to form ethylene gas (14-16). However, it is difficult to determine the structure of the products formed on the Li-metal surface with XPS alone.

For the LiBOB experiments, the 200 mM LiI sample exhibited these mysterious high binding energy peaks on C 1s as well (**Figure 20**b (iii). Peaks seen in yellow, red and green (on far left) as they are assigned in **Table 3**. High resolution spectra of N 1s is missing for that sample, but from their survey spectra (**Figure 21**b) it is possible to make an assumption that the same pattern arises on N 1s, compared to **Figure 14b**. Except there is no $LiNO_3$ peak at 407.8 eV, since in this case $LiNO_3$ was substituted for LiBOB. Furthermore, the amount of time that the Li-metal was in the electrolyte varies for these two.

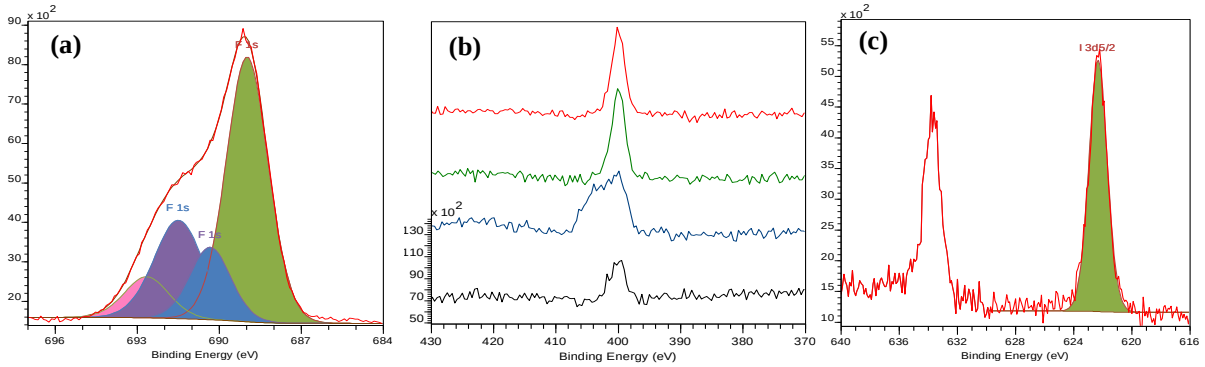

Figure 21: XPS spectra of Li-metal immersed in electrolyte for 13 days. a) F 1s b) N 1s, **Red**: No LiI; **Green**: 100 mM LiI; **Blue**: 200 mM LiI and **Black** 500 mM LiI c) I $3d_{5/2}$. Electrolyte for a-c) contained 1.0 M LiTFSI, 0.20 M LiBOB and 200 mM LiI in DOL:DME. (1:1 by w.). Peaks are depicted in table 3.

The I $3d_{5/2}$ spectra exhibits no peaks (**Figure 21**c) at 621.4, 623.2 and 624.8 eV. This would indicate that the sample does not exhibit an iodine bonded to carbon, nor any traces of I_2O_5 or $LiIO_3$ (**Table 3**). The chemistry is different, since $LiNO_3$ was substituted for LiBOB.

The B 1s XPS exhibited a single peak at 193.0 eV within the SEI layer.[20] This indicates that LiBOB is stable (does not decompose) during the first 13 days of dipping (**Figure S2**). However, further investigation is needed to observe whether LiBOB decomposition products form over longer time periods or not. LiBOB as an additive exhibits a more consistent trend, in terms of the C-C:C-O peak area ratio (**Figure 16**), in contrast with $LiNO_3$ as an additive. Furthermore, LiBOB exhibits a trend similar to $LiNO_3$ (**Figure 15**). After 13 days immersed in the electrolyte, the C-C:C-O pattern emerges. The LiBOB peak on B 1s decreases as more LiI is added (**Figure S2**). Therefore, the same conclusion can be made as was done for **Figure 15**.

It is reported that LiTFSI, $N(SO_2CF_3)_2$ forms various decomposition products[1] (**Figure 22**) on the Li-metal surface. At least one of them has already been mentioned and identified in this thesis, LiF.

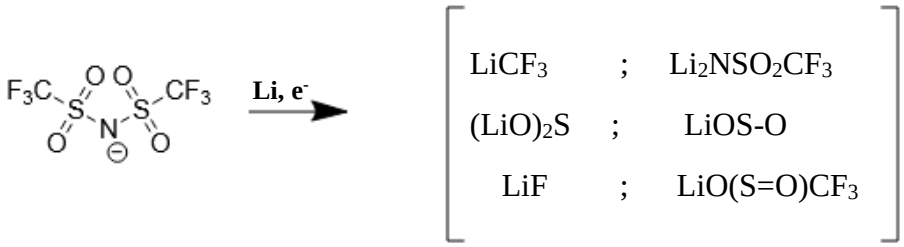

Figure 22: Li-metal surface reacting with DOL-LiTFSI and its decomposition products.

Identifying some of these species (**Figure 22**) with absolute certainty is difficult. There is a lack of information available in the science community in terms of XPS peak references. Furthermore, some of them might even appear at the same or similar binding energies as the original salt and would therefore be difficult to assume the origin.

4.4 SEM analysis of LiTFSI based electrolytes

SEM and EDS analysis revealed some quite interesting features on the Li-metal surface. The Li-metal was immersed in electrolyte solution for 5 days. The surface film inhibits a lot of line cracks, as can be seen especially in **Figure 23**d. Solvents that are typically used in Li-S batteries have low viscosity and will easily penetrate the formed film to reach the fresh Li-metal through the cracks.

If one were to use this Li-metal sample in **Figure 23**, one would expect a lot of dendrites to grow on the bare lithium sites. The darker grey areas between the cracks (**Figure 23**d) is assumed to be bare lithium metal. The patchiness could be because surface roughness is rather high. Meaning that if the Li-metal surface was flattened with some sort of rolling technique, one might get a more uniform SEI formation across the surface.

EDS was conducted on a certain area of the Li-metal foil. The only elements that could be detected were the following in **Figure 24**. Surprisingly, iodine could not be detected, which is rather odd, since its signal was reasonably intense on XPS. Due to the low atomic number of lithium, it could not be detected via EDS. However, there is a possibility that lithium dendrite formed on the uncycled Li-metal foil. From combining all the elemental EDS spectra (**Figure 24**a-e), dark areas appear throughout the surface. The dark areas are where no elements could be detected. Therefore, it is assumed that they are lithium dendrites. The most apparent one

would be the dark spot in the upper right corner for all the elements (**Figure 24**a-e), as indicated by the yellow arrow on **Figure 24**f.

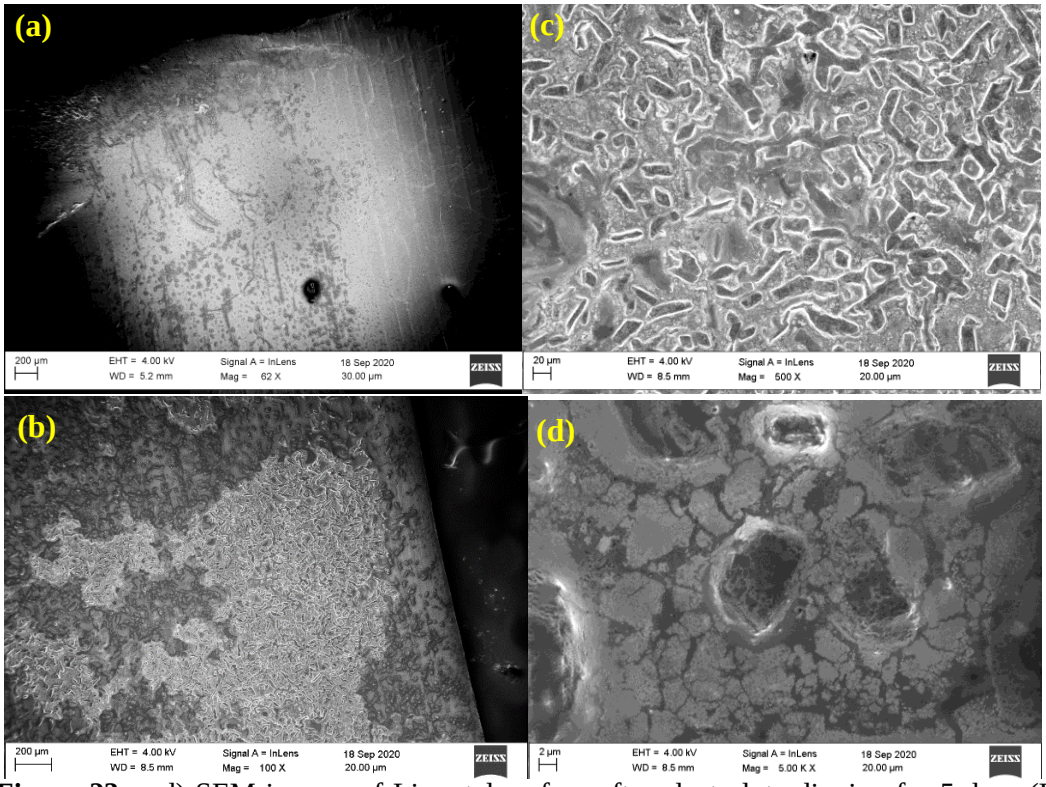

Figure 23: a-d) SEM images of Li-metal surface after electrolyte dipping for 5 days (LiTFSI 1.0M; LiBOB 0.20 M; LiI 0.50 M in DOL:DME (1:1 by w.)).

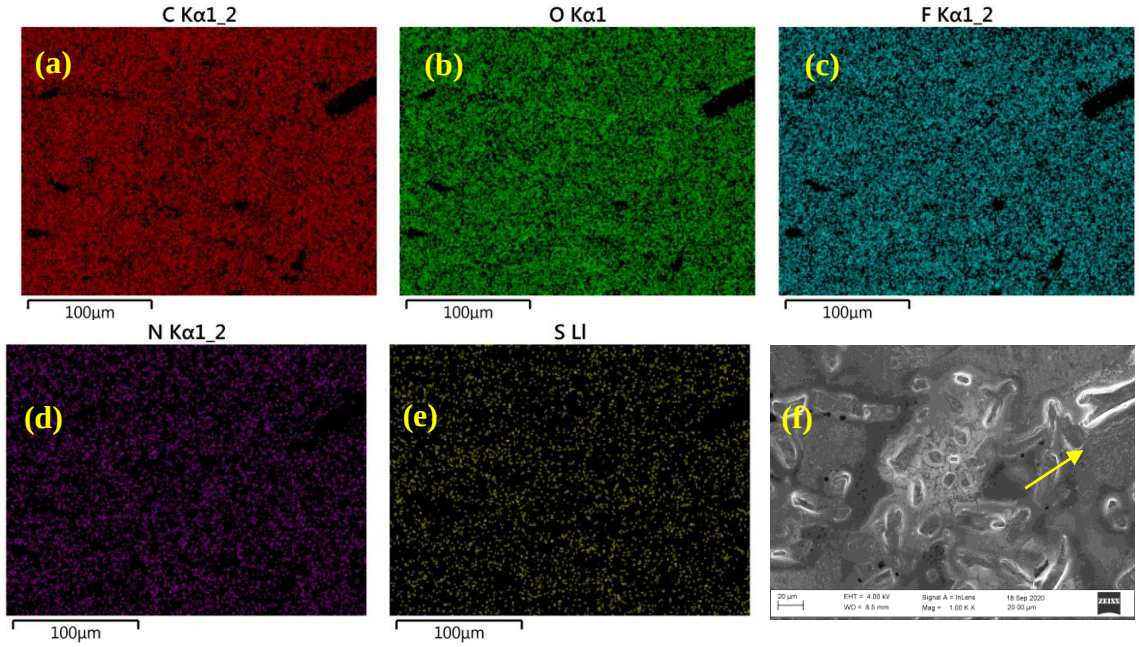

Figure 24: EDS of Li-metal surface after electrolyte dipping for 5 days (LiTFSI 1.0M; LiBOB 0.20 M; LiI 0.50 M in DOL:DME (1:1 by w.)). a) Carbon – C b) Oxygen – O c) Fluorine – F d) Nitrogen – N e) Sulphur – S, and e) SEM of same location on sample as in a-e)

5. Conclusion and outlook

Once the samples are being analyzed via XPS, it was important to be aware of that the surface may not be uniform across the whole surface. To make sure that reliable results had been obtained, a scanning of multiple locations would give a better idea of whether a stable and compact surface film had been detected. If a prevailing pattern were detected, one could proceed with that location. When it was impossible to achieve such consistency with a single sample, the wisest thing to do was to repeat by washing a fresh sample. The 500 mM LiI samples were the easiest ones to analyze, since they appeared to have a more stable and uniform SEI, while the 100 and 200 mM LiI ones were trickier and had to be repeated more often.

Many of the species, such as the multiple peaks at the higher binding energy range of C 1s (>294 eV) and F 1s (>690 eV) could not be identified. The most likely explanation would be a charging effect, causing a shift in peaks to higher binding energies. Other peaks, which have been reported, were easier to identify, such as $-CF_3$, CO_3^{2-}, NO_3^{2-} and LiF.

The SEM and EDS revealed that there was most likely Li dendrite on the Li-metal surface, even though it was never cycled. This could also mean that the morphology of the Li-metal was already dendritic before it was immersed in the electrolyte solutions. There was also a strong indication of a uniform film having formed and then cracked after being dried. The film could also have cracked from mounting the Li-metal foil onto the sample holder. The 500 mM LiI sample was the sample of choice due to its high stability and uniformity in XPS.

To compare the $LiNO_3$ and LiBOB additives is difficult at this point. The $LiNO_3$ experiments seemed to form at least one reductive decomposition product (NO_2^-) after 20 days, while LiBOB was stable throughout its 13 days. LiTFSI seemed to decompose with the same manner in both $LiNO_3$ and LiBOB. Lithium iodide (LiI) exhibited decomposition products, such as IO_3 and I_2O_5, according to the I $3d_{5/2}$ spectra.

The C-C:C-O ratio exhibited a consistent trend for the LiBOB experiments in section 4.3. As a matter of fact, the ratio increases as more LiI is added to the electrolyte solution. This could indicate that the SEI has been altered. Polymerization of the solvent, such as DME, is a possibility. Furthermore, the peak intensities for $LiCO_3$ (C 1s), LiTFSI (C 1s), $LiNO_3$ (N 1s) and LiBOB (B 1s) were lower as more LiI was added to the electrolyte solutions. These trends could indicate that a layer is formed on top of these beforementioned species. This could also mean that LiI prevents these species from forming on the Li-metal in the first place. Therefore,

LiI could work as an additive to control how much of the salts/additives react or form on the Li-metal surface.

Such thorough XPS studies with LiI as an additive for Li-metal anodes has never been published before, which made this research project even more challenging. Furthermore, unidentified chemical species need further investigation. Especially the LiTFSI and LiI decomposition products. Cycling experiments in parallel with XPS analyses would be the next step, to gain greater insight of decomposition products formed on the Li-metal surface. Certain rolling techniques, mentioned in section 1.3.1, would be interesting to demonstrate on the Li-metal. This might decrease the inhomogeneousness across the Li-metal surface.

6. References

1. D. Aurbach et al., *Journal of Electrochemical Soc*iety, **156**, A694-A702 (2009).
2. S. Jiao et al., *Joule*, **2**, 110–124 (2018).
3. A. Rosenman et al., *Advanced Energy Materials*, **5**, 1500212 (2015).
4. X.-B. Cheng et al., *Journal of Electrochemical Soc*iety, **165**, A6058–A6072 (2017).
5. J. Scheers et al., *Journal of Power Sources*, **255**, 204–218 (2014).
6. H. Zhao et al., *Chemical Engineering Journal*, **347**, 343–365 (2018).
7. Y. Liu, B. Li, J. Liu, S. Li, and S. Yang, *Journal of Materials Chemistry A*, **5**, 18862–18869 (2017).
8. Q. Li et al., *Advanced Functional Mater*ials, **27**, 1606422 (2017).
9. K. Yan et al., *Nature Energy*, **1**, 1 (2016).
10. D. Lin et al., *Nature Nanotech*, **11**, 626–632 (2016).
11. Q. Ma et al., *Journal of Electrochemical Soc*iety, **163**, A1776–A1783 (2016).
12. X.-B. Cheng et al., *Advanced Sci*ence, **3**, 1500213 (2015).
13. F. Kita et al., *Journal of Power Sources*, **90**, 27–32 (2000).
14. F. Wu et al., *Advanced Materials*, **27**, 101–108 (2014).
15. J. R. Owen, *Chemical Society Rev*iews, **26**, 259 (1997).
16. D. W. McOwen et al., *Energy & Environmental Sci*ence, **7**, 416–426 (2014).
17. A. Einstein, *Annalen der Physik*, **322**, 132–148 (1905).
18. J.F. Moulder et al., *Handbook of X-ray Photoelectron Spectroscopy*, Physical Electronics Inc., Eden Prairie (1995).
19. A. Klein et al., *Bunsenmagazin*, **10**, 124–139 (2008).
20. Schreifels J.A. et al., *Journal of Catalysis*, **65**, 195-206 (1980).
21. S.P. Kowalczyk et al., *Solid State Communications*, **23**, 161–169 (1977).
22. S. Tougaard, *Physical Review B*, **34**, 6779-6783 (1986).
23. S. Doniach et al., *Journal of Physics C: Solid State Phys*ics, **3**, 285–291 (1970).
24. E. Yoo et al., *Journal of Materials Chem*istry A, **7**, 18318–18323 (2019).
25. Q. J. Meisner et al., *Journal of Electrochemical Soc*iety, **167**, 070528 (2020).
26. [No Author], (2017) https://www.chemicalbook.com/ChemicalProductProperty_EN_CB8688141.htm. Retrieved 2020-03-20.
27. M. Valvo et al., *ChemSusChem*, **10**, 2431–2448 (2017).
28. A. Herrera-Gomez et al., *Surface and Interface Anal*ysis, **46**, 897–905 (2014).

29. M. C. Biesinger et al., *Applied Surface Science*, **257**, 889 (2010).
30. M. R. Busche et al., *Nature Chemistry*, **8**, 426–434 (2016).
31. N. Plylahan et al., *Nanoscale Research Letters*, **9**, 544 (2014).
32. G. Greczynski et al., *Progress in Materials Science*, **107**, 100591 (2020).
33. H. S. Munro et al., *Journal of Polymer Science Part A: Polymer Chemistry*, **28**, 923–929 (1990).
34. Y. An et al., *Electrochimica Acta*, **56**, 4841-4848 (2011).
35. S. Xiong et al., *Ionics*, **18**, 249–254 (2011)
36. Beamson G et al., *High Resolution XPS of Organic Polymers: the Scienta ESCA300 Database*, Wiley, New York, NY, (1992).
37. S. Xiong et al., *Electrochimica Acta*, **83**, 78–86 (2012).
38. C. Yan et al., *Angewandte Chemie International Edition*, **57**, 14055–14059 (2018).
39. D. K. Smith et al., *Physical Chemistry Chemical Physics*, **18**, 11243–11250 (2016).
40. W. Jia et al., *ACS Applied Materials & Interfaces*, **9**, 7068–7074 (2017)
41. S. Dierks, (1995) https://web.archive.org/web/20080309151355/http:/www.espimetals.com/msds's/lithiumiodide.pdf. Retrieved 2020-03-20.
42. J. P. Simmons et al., *Journal of American Chemical Soc*iety, **49**, 701–703 (1927).
43. G. Leverick et al., *Joule*, **3**, 1106–1126 (2019).
44. M. Liu et al., *Nano Energy*, **40**, 240–247 (2017).
45. [No Author], (2017) https://www.energy.gov/eere/articles/how-does-lithium-ion-battery-work. Retrieved 2020-09-20.
46. R. Borah et al., *Materials Today Advances*, **6**, 100046 (2020).
47. J. Garche et al., *Li-battery safety*. Elsevier, Amsterdam, Netherlands, (2019).
48. R. Wang et al., *Journal of Energy Chemistry*, **48**, 145–159 (2020).
49. X.-B. Cheng et al., *ACS Energy Letters*, **3**, 1564–1570 (2018).
50. J. Becking et al., *Advanced Materials & Interfaces*, **4**, 1700166 (2017).
51. Y. Mekonnen et al., *SoutheastCon 2016*, 1-6 (2016).
52. D. Puthusseri et al., *ACS Omega*, **3**, 4591–4592 (2018).
53. X. Chen et al., *Energy Storage Materials*, **8**, 194–201 (2017).

7 Appendix

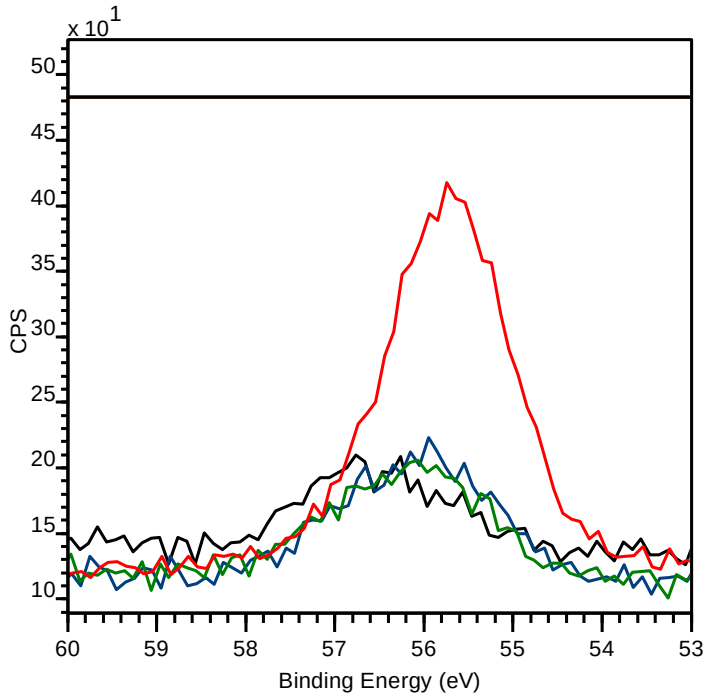

Figure S1: Li 1s XPS spectra of Li-metal foil immersed in electrolyte (1.0 M LiTFSI; 0.25 M $LiNO_3$ in 1:1 DOL:DME by weight) for 72 hours. Red: No LiI; Green: 100 mM LiI; Blue: 200 mM LiI; Black: 500 m M LiI. Single peak distinctive for Li(0) at ~56 eV.

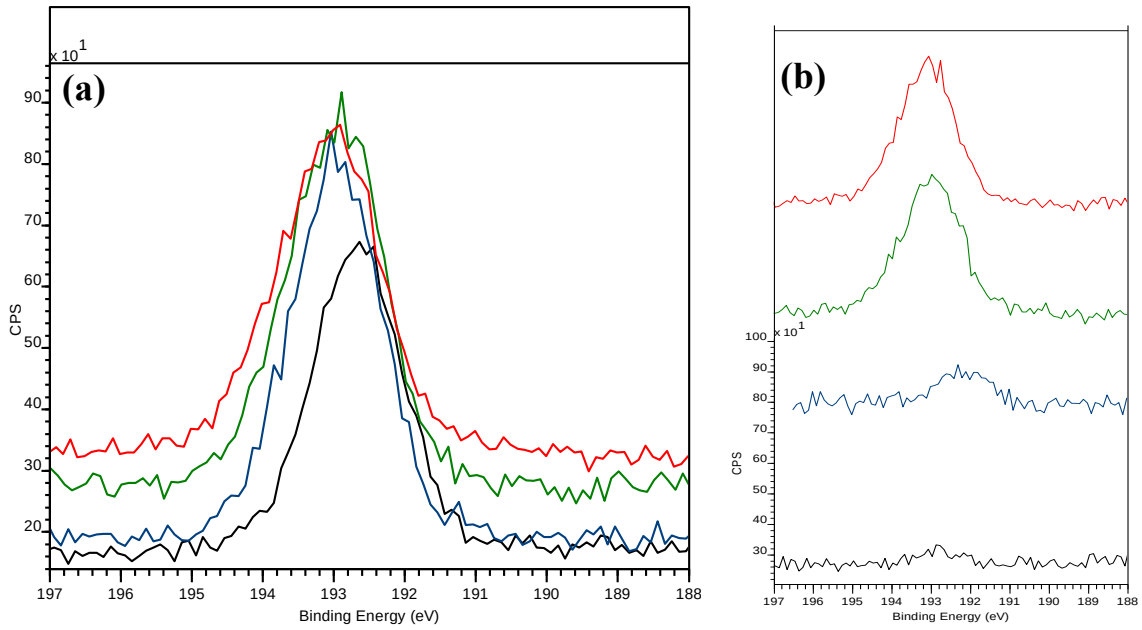

Figure S2: B 1s XPS spectra of Li-metal foil immersed in electrolyte (1.0 M LiTFSI; 0.20 M LiBOB in 1:1 DOL:DME by weight) a) for 5 days. b) 13 days. **Red**: No LiI; **Green**: 100 mM; **Blue**: 200 mM; **Black**: 500 mM LiI. Single peak, distinctive for LiBOB at ~193 eV.